Chapter 5
Modeling Plant Growth: Deterministic Case

Philippe De Reffye, Ep Heuvelink, Véronique Letort, and Mengzhen Kang

Abstract This chapter introduces a detailed mathematical model for simulating plant growth, with a focus on integrating physiological crop models to accurately represent biomass production and distribution. The GreenLab model allows for the analysis of individual plant growth at the phytomer level, reconstructing the plant's three-dimensional (3D) architecture from a two-dimensional (2D) planar structure formed by meristem function. Based on a source-sink functioning process, organs within the model are assigned specific roles in biomass production and allocation. The model calculates the biomass demand by evaluating the sink strength of organs produced per cohort, considering their physiological and chronological ages. The model uses a recurrence mechanism starting from the seed to track the growth and development of plants over time. The integration of allometric relationships ensures that the organ morphology is consistent with their functional roles. The use of physiological age allows to decompose the plant structure in separated pieces of phytomer axes, known as organic series. Organic series contain the plant growth memory. The organic analysis method infers growth parameters from plant

P. De Reffye
CIRAD, UMR AMAP, Montpellier, France

AMAP, Univ Montpellier, CIRAD, CNRS, INRAE, IRD, Montpellier, France

E. Heuvelink
Horticulture and Product Physiology, Wageningen University and Research, PB, Wageningen, The Netherlands
e-mail: Ep.Heuvelink@wur.nl

V. Letort
Mathématiques et Informatique pour la Complexité et les Systèmes, CentraleSupélec-Université Paris-Saclay, Gif-sur-Yvette, France
e-mail: veronique.lechevalier@centralesupelec.fr

M. Kang (✉)
State Key Laboratory for Multimodal Artificial Intelligence Systems, Institute of Automation, Chinese Academy of Sciences (CASIA), Beijing, China

School of Artificial Intelligence, University of Chinese Academy of Sciences, Beijing, China
e-mail: mengzhen.kang@ia.ac.cn

P. De Reffye et al. (eds.), *Plant Model Greenlab for Botany and Agronomy*,
https://doi.org/10.1007/978-981-97-7541-5_5

architecture, aiding in data restoration. This mathematical model not only bridges the gap between functional–structural and physiological crop models but also provides a practical approach to crop production and agronomic applications.

Keywords Crop models · Photosynthesis · Source-sink functioning · Growth equations · Cohorts · Organic series · Free and limited growth

5.1 Introduction

This chapter aims to put plant growth into mathematical equations. In this approach, particular attention is paid to staying as close as possible with physiological crop models, to keep strong compatibility. These models are usually photosynthesis driven and calculate the biomass produced by a plant stand and its distribution in organ compartments (leaves, internodes, fruits, roots, etc.). Mathematical modeling in GreenLab makes it possible to study plants at the level of the architecture of the individual plant, and more precisely at the level of the phytomer and the organs. The stand becomes a set of phytomers composed of organs distributed over a set of plants.

The architecture of a plant is reconstructed in three-dimensional (3D) using geometric operators from a two-dimensional (2D) planar structure, which is generated by the functioning of meristems. This structure is created using scaled objects representing the organs (Chaps. 4 and 14). These organs are now assigned functional roles in terms of biomass production and distribution to calculate plant growth. Biomass is synthesized by leaves (source organs) and then distributed to all the functioning organs belonging to the plant architecture (sink organs). There are new organs created in the structure, as well as old ones that continue to expand in volume (including leaves). By feedback, the updated leaf area increases the plant's growth. The plant development model resulting from the functioning of meristems (Chap. 3) makes it possible to calculate the number of organs produced per cohort (being defined as a layer in plant crown composed of organs of the same physiological and chronological ages), to obtain the "biomass demand" of the plant by considering their sink strength. The system works by recurrence from the seed. The morphology of organs depends on their biomass, density, and shape coefficients (allometries). The architecture of the plant produced by simulating the growth is not visually different from that provided by simulating the development with empirically pre-scaled organs. However, the organs now play their functional roles. This allows a new approach to crop production and new agronomic applications.

5.2 Basic Biological Processes of Plant Growth and Production

The growth of a plant is dependent on two biological processes that interact:

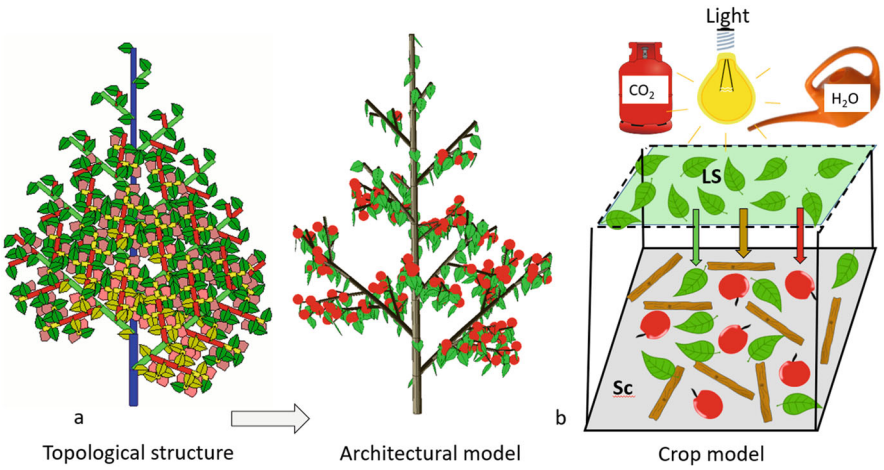

Fig. 5.1 Architectural plant model and physiological crop model. (**a**) Architectural model for development, a topological representation of the planar structure of a plant with different types of axes corresponding to several physiological ages (PAs) (4 here, represented by the blue, green, red, and yellow color, respectively). The architecture of the plant is obtained by giving the botanical entities their geometric positions, shapes, and dimensions. (**b**) Physiological crop model for growth and interception of light by a plant canopy. Plants are not considered as individuals: what matters is the ratio between the active leaf surface (*LS*) and the ground area (*Sc*). The biomass produced is distributed in proportion in different plant compartments according to their sinks (leaves, internodes, and fruits) without knowing the position of the organs in the plant structure

- Development, which builds the leafy axes to form a topological structure (Fig. 5.1a) and depends on the functioning of meristems. Botany studies plant architecture as a composition of different types of axes, whose combination generates architectural models (Hallé et al. 1978). The plant is considered as an individual, and its architecture is seen as the result of a morphogenetic program, which does not interact much with the climatic environment in the absence of stress. Photosynthesis is ignored in this process.
- Growth, which depends on photosynthesis through the interaction of source–sink relationships among organs and causes organ expansion. Agronomy studies the production of a stand per unit area, using physiological crop models involving environmental factors and the interception of light by foliage. The plant is not considered as an individual in this context (Fig. 5.1b). The different types of organs are grouped into compartments (e.g., leaves, stems, fruits) at the plant stand level, expressed per unit ground area (often 1 m^2). Stand growth is, therefore, the result of both biomass produced per unit area and time, and its distribution into the various plant compartments.

The modeling approach described in this book (GreenLab model) synthesizes the two approaches by combining botanical architectural models with agronomic crop models to produce a computational plant model adapted to the needs of agriculture.

5.2.1 Axis Elongation and Thermal Time

Plant growth fluctuates as a result of variations in environmental factors (light, temperature, etc.). The elongation of the axes is irregular when measured according to the "calendar time" (days). It depends not only on the functioning of the meristems that create new phytomers but also on their expansion. If the temperature drops, the elongation slows down. Agronomists observe that the cumulative number of phytomers created by a meristem on a stem is a linear function of the sum of the daily average temperatures (called "thermal time") received by the crop. Each created phytomer corresponds to a development cycle (DC). The study of physiological crop models is then greatly simplified using thermal time, as the development rate becomes more stable.

While it seems relevant to discretize the developmental stages of a plant whose meristems produce integer numbers of phytomers in cycles, on the other hand, the expansion in organ volume remains continuous and has no explicit marker of time. The growth time of the organs, however, is related to the thermal time as for the development of the axes. The expansion of organs that depends on photosynthesis slows down when the temperature drops. The expansion duration of the organs also stabilizes when the thermal time is used as the unit of measurement instead of the calendar time. To synchronize growth and development in the plant's functioning, the GreenLab model uses the development cycle (DC) as a modeling time unit. The growth cycle (GC) is then equal to the development cycle (DC). In each cycle, meristems initiate new phytomers, and leaves produce biomass that is distributed in the plant according to the competition among different sink organs. This method makes it possible to monitor the growth of a plant, even when its development stops with the terminal flowering of the stem, as in the case of wheat, sunflower, and maize (Guo et al. 2006) (Fig. 5.2). The linear relationship between the number of cycles and thermal time is established during the development stage when phytomers accumulate, and then extrapolated beyond.

The plant's functioning is thus synchronized for development and growth.

5.2.2 Photosynthesis and Biomass Production

The fresh biomass (fresh matter) of the organs consists mainly of water (80–95%) absorbed from the soil, and dry matter (5–20%) mainly derived from photosynthesis, A small part of the dry matter consists of minerals necessary for physiological functioning (nitrogen, phosphorus, potassium, iron, etc.) but negligible in weight.

The dry biomass (dry matter) of the organs consists of the part of the fresh biomass, which remains when all its water content is removed by desiccation.

Biomass production depends mainly on environmental factors: light, temperature, water, and CO_2 concentration of the air.

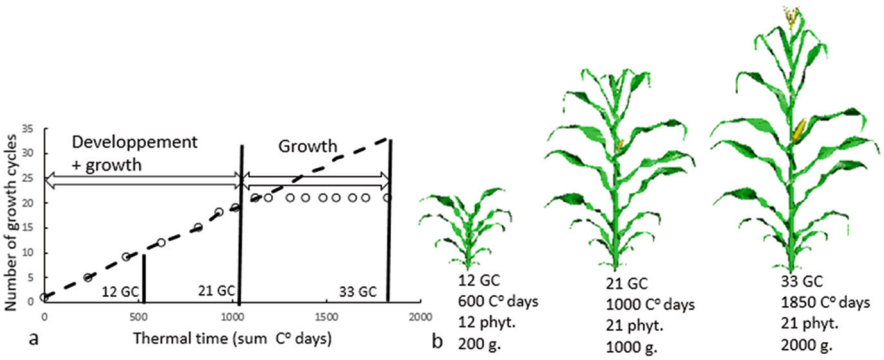

Fig. 5.2 Synchronization of growth and development cycles. Observations on the development and growth stages of a maize plant grown in China. "o" represents the number of observed phytomers at different stages of growth, "—" represents number of theoretical growth cycles (GC). Source: Ma Yun-Tao, Chinese Agricultural University (CAU). (**a**) The duration of the first stage is between germination and the formation of the terminal tassel, which stops the production of new phytomers but not the growth in cycles. During this period, a linear relationship between thermal time and the number of cycles is established, which is equal to the number of phytomers. In the second period, the relationship is extrapolated to the duration of the growth in the number of cycles. Note that the biomass produced doubles after the development has stopped. (**b**) Three growth stages of 12, 21, and 33 development cycles (DCs) are shown, with the corresponding number of phytomers, temperature sum, and weight of plants

The raw sap composed of water and mineral salts is extracted from the soil by the roots. By a physical phenomenon of suction, water is sucked through the xylem vessels to the surface of the leaves, where 90% of its volume evaporates. The remaining 10% contributes to the plant's fresh biomass. Sugars (assimilates) from photosynthesis are distributed to the organs to ensure their growth through specialized channels throughout the plant (phloem).

The activity of photosynthesis depends on the energy carried by the light and the surface of the foliage that intercepts it. de Wit (1978) firstly put forward the relationship between the biomass produced per m^2 of plants per day and the incident light energy:

$$\mathrm{Q(t)} = C \cdot \mathrm{PAR}(t) \cdot (1 - \exp(-k \cdot \mathrm{LAI}(t))) \cdot \Delta t \tag{5.1}$$

where $Q(t)$ is the dry biomass produced by the stand on day t during the period Δt; PAR (t) (photosynthetically active radiation) is the amount of the sun's radiation that can be used for photosynthesis, measured in megajoules (MJ)/time unit/m^2; C is the light use efficiency (a conversion coefficient); k is the light extinction coefficient, a coefficient depending on the horizontality of the leaves; LAI, called leaf area index, is the leaf area (m^2) of the stand of plants per m^2 of ground area. The function $(1 - \exp(-k \cdot \mathrm{LAI}))$ is derived from Beer-Lambert's law, which calculates the fraction of light intercepted by the foliage. It allows the overlapping rate of the leaves within the

canopy to be considered in the calculation of photosynthetic production. This limits the interception of light by the leaf surface. The function gives the percentage of ground area shadow by the foliage per m^2. For LAI > 3, the plant intercepts almost all incident light. In the absence of stress (thermal, water), light use efficiency is a constant for a species.

For tomato cultivation in the Netherlands, Heuvelink (2006 personal communication) states that the overall radiation received by the stand in summer averages 17 MJ/m^2 per day; but only 50% of the radiation (PAR) is usable for photosynthesis and this rate decreases by a further factor of 0.7 if the plant is grown in a greenhouse, as light must pass through the greenhouse cover. The radiation received by the stand is therefore calculated as: $17 \times 0.5 \times 0.7 = 6.0$ MJ/m^2 per day. In winter, the global radiation drops to 2 MJ/m^2 per day, which is why supplemental lighting is necessay.

Since the temperature is controlled (≈ 20 °C) in modern greenhouses, it is usually not a limiting factor.

Beer Lambert's law of light extinction is generally well verified in greenhouse crops (Fig. 5.4).

The LAI is high during the production period: LAI > 3, so $(1 - \exp(-3 * 0.7)) \cong 0.9$, which means that about 90% of the light is intercepted by the foliage (with $k = 0.7$, typical for a horticultural crop).

A typical value for the light use efficiency of a tomato stand is 3 g/MJ PAR. It is stable and does not depend on the planting density. But it is a value that can change depending on the climatic factors in the greenhouse (e.g., about 30% higher at 1000 ppm CO_2 compared to 400 ppm CO_2).

We deduce from this that the crop production of dry matter per m^2 for a tomato stand in summer in a Dutch greenhouse is: $Q = 3 \times 6 \times 0.90 \approx 16$ g/m^2/day.

This value also depends on the plant species, but an order of magnitude of $Q \approx 20$ g/m^2 per day of dry matter is reasonable for the dry mass increase of a canopy in general in summer, which gives at a dry matter content of 6%: $Q \approx 270$ g/m^2/day for the synthetized fresh matter.

If we consider the planting density d and a k·LAI > 3 that produces a quantity Q of biomass per m^2 independent of the planting density, each plant will grow on average each day by an amount q inversely proportional to d: $q = Q/d$. The more plants there are, the more they are reduced, the limiting factor is the maximum production Q of the stand per unit area that does not depend on LAI and thus of planting density.

Figure 5.3 gives the effects of temperature and light on plant development and growth.

A genetic program controls step by step the functioning of the meristems to generate architectural development. In Fig. 5.3, after five repetitions of the same phytomer, the meristem transforms into a flower. The higher the ambient temperature, the faster the plant develops. The more incident light the plant receives, the bigger it grows.

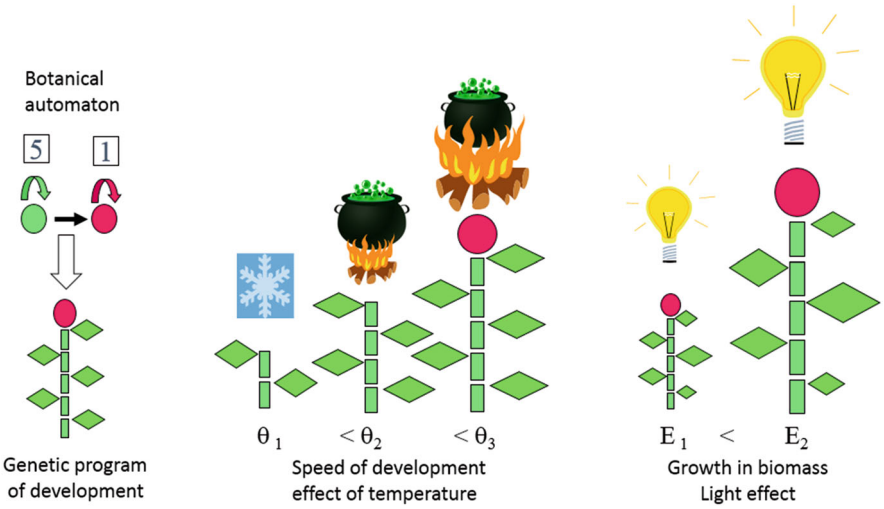

Fig. 5.3 Effect of light and temperature on plant development and growth

5.2.3 Common Pool

5.2.3.1 Use of Sugars by the Plant

Photosynthesis produces sugars (assimilates) that serve both as components and as combustible materials for the plant system. Before being used and distributed to the plant's organs, the synthesized sugars are initially stored in a virtual tank called a *common pool*.

Once transformed into cellulose, they constitute the cellular walls of the plant that build its structure. They form the largest proportion of the plant's dry matter. This material, once produced, no longer participates in metabolic processes; it is referred to as fixed carbon. When converted into starch, these sugars are stored as reserves within the vacuoles of the cells, appearing as grains. They are used for physiological functions of the plant system (transport of sugars in the structure, respiration), supplying the energy necessary for growth.

In a favorable environment, the proportion between the component and the combustible is stable. Depending on the type of component, the production cost is different. For instance, synthesizing oil requires twice as much sugar as producing cellulose, on a weight basis.

In this book, we focus only on "net photosynthesis," which refers to the portion of cellulose-derived sugars that contribute to produce the plant's architecture within a stable climatic environment.

5.2.3.2 Storage of Sugars by the Plant

The expansion of the organs in volume is ensured by their access to the sugars produced by photosynthesis. To simplify, everything happens as if a common biomass pool that is directly accessible by the organs. The notion of a pool has the advantage of not having to simulate the transport of the material produced by the leaves throughout the structure to feed the organs via the network of branches. The computer simulation of this transportation is costly in terms of calculation time. The assumption of a common pool has been validated as a good approximation and is frequently used in physiological crop models.

The plant's organs are divided into two categories:

- *Source organs:* They produce biomass through photosynthesis by intercepting light at their surface, using intracellular organelles called chloroplasts. These organs are also sinks because they are made of fresh biomass. The leaf is the main source organ. Its flattened shape optimizes light interception. Other organs may also be involved in photosynthesis, such as the sheaths of grass leaves, pods of legumes, siliques of cruciferous plants, and even young internodes. At the origin of growth, the seed is the initial source organ. As they become senescent, the organs can return part of their biomass to the common pool and thus become sources again: this is the process of remobilization. Organs like tulip bulbs or potato tubers are source organs at the start of cultivation.
- *Sink organs*. All organs (even leaves) are sinks that attract the produced biomass. The sink strength of an organ corresponds to the extent of its needs to sustain its expansion. It varies according to its type and developmental stage. In general, the sink strength increases from the creation of the organ to a maximum, then decreases and finally becomes null when the organ reaches maturity. Some sinks are particular: the woody rings of the leafy axes at the origin of secondary growth, and the roots. In GreenLab, the latter is simulated as a mere compartment because they cannot be sufficiently detailed. Another hidden sink is the reserve compartment consisting essentially of starch grains stored in the cells.

The geometrical shape of an organ is dependent on its volume (which depends on its weight and density) and on shape coefficients called allometries:

- The leaf is considered as a flattened volume whose thickness ε is constant. The surface is in these conditions proportional to the volume;
- The internode is considered as a cylinder defined by the surface of its section s and its height h. Its volume v ($v = h{\cdot}s$) depends on the quantity of biomass q and the density d: $v = q/d$; the shape coefficient β characterizes the elongation of the cylinder, and the coefficient γ is the allometry between s and h according to the relationship: $h/s = \beta{\cdot}v^{\gamma}$. The dimensions of the cylinder are then linked to the volume and allometries:

$$h = \sqrt{\beta} \cdot (v)^{\frac{1+\gamma}{2}}$$

$$s = \sqrt{\frac{1}{\beta}} \cdot (v)^{\frac{1-\gamma}{2}}$$

$$v = h \cdot s \tag{5.2}$$

Finally, to simplify, we can assume a fruit to be an ellipsoid, the half axes being the shape coefficients.

5.3 An Example of a Physiological Crop Model: TomSim

Numerous agronomic experiments on tomato have been carried out to identify the rules that underly the functioning of the TomSim model (Heuvelink 1995, 1996a, b). The production modeling is based on Eq. (5.1). The leaf area index (LAI) and compartment weights are recorded during crop growth.

5.3.1 Light Interception by the Canopy in the Greenhouse

The stability of light use efficiency and the validity of the law of light interception (Beer-Lambert) are well verified in the tomato experiments underlying TomSim. The LAI determines production per m^2 (Fig. 5.4).

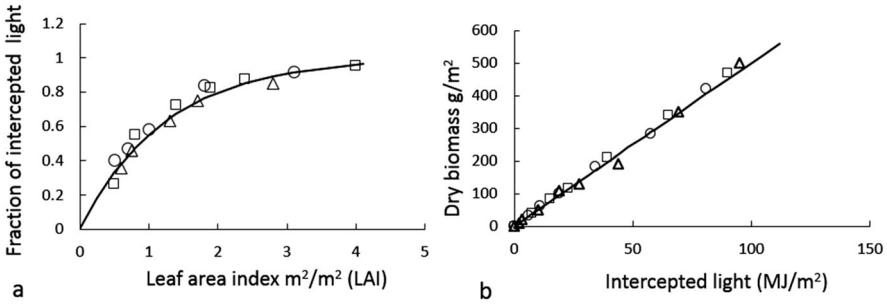

Fig. 5.4 (**a**) The computation of the light interception with Beer-Lambert's law for a chrysanthemum population of three planting densities. (**b**) Under the same conditions, the biomass production by the stand is proportional to the cumulative intercepted light. The light use efficiency (LUE) was determined to be five g·DM/MJ/PAR. The markers correspond to the measurements (three different planting densities) and the curves represent the theoretical values. (Source: Ep Heuvelink, Wageningen University)

5.3.2 *Effect of Planting Density on the Individual Plant and Population Growth*

The reference cultivated area for production is a square meter (m^2). At low-density ranges, increasing the planting density obviously produces more biomass per m^2, because the canopy of plants has not yet closed. We see that production is growing exponentially. As soon as the LAI becomes large (greater than 3), the biomass production per m^2 is hardly dependent on planting density (Fig. 5.5a). Individual plants tend to have a weight that is inversely proportional to the planting density (Fig. 5.5b).

Another representation of the effect of planting density on the single plant and on the stand is illustrated below (Figs. 5.33 and 5.34).

5.3.3 *Effect of Biomass Partitioning on the Growth*

During tomato growth, Heuvelink carried out controlled fruit removal in the bunch to observe the effect on total biomass production for the population (Fig. 5.6). In all these experiments, an LAI of more than 3 was obtained. If the harvest index (HI) depends on the number of fruits per bunch, the total biomass production per m^2 is invariant because it is the LAI that controls the total biomass production (Eq. 5.1) and not the partitioning of the biomass.

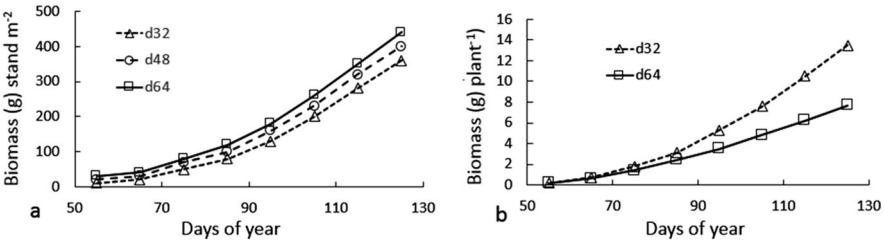

Fig. 5.5 Effect of planting density on individual and population growth. (**a**) Growth of a chrysanthemum population at three planting densities (32, 48, 64 plants/m^2): at the beginning, it is the total leaf area that counts and the growth is exponential. Biomass production per m^2 obviously increases with the density. After about 90 days, growth becomes nearly linear and close for the three densities (parallel lines) because the plant canopies are all closed. The LAI is high, and the ground surface is completely covered with the foliage. It is then the m^2 that produces and is no longer the sum of the surface area of the leaves. (**b**) Growth of an individual plant for two densities (32, 64 plants/m^2). A plant with a density of 64 plants/m^2 (□) weighs as much at the beginning of growth as a plant with a density of 32 plants/m^2 (Δ), because the plants are isolated from each other. At the end of the cultivation, plant weight is almost twice as high for the widest spacing (roughly the same total biomass per m^2 (panel a) but only half the number of plants). (Source: Ep Heuvelink, Wageningen University)

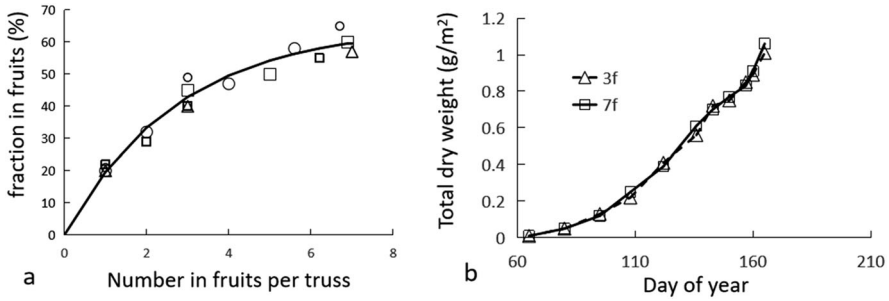

Fig. 5.6 (**a**) Harvest Index (HI) (% fruit weight/plant weight) for greenhouse tomato crops grown for a period of about 100 days starting at the anthesis of the first truss, as a function of the number of fruits per truss for three planting densities. At low numbers of fruits per truss, HI is proportional to the number of fruits, and it saturates at a maximum of 60% of the plant's weight. (**b**) Total weight of the plants at two different fruit loads. The number of fruits per truss has no influence on the total weight of the plants. This is because at both fruit loads LAI was high (LAI >3), so total biomass production was the same, and only partitioning is influenced by the fruit load. (Source Ep Heuvelink, Wageningen University)

This phenomenon is found in the production of cucumbers and peppers. Many fruit abortions cause the HI to vary greatly over time. But since the LAI is high, biomass production is constant as light interception is saturated (i.e., at its maximum). The biomass of the compartments varies in a complementary way, under the constraint that their sum (the total biomass of the plant) is constant.

It should be noted that if the fruit is removed in some plants, there may be physiological reactions. Thus, if the ear of maize is removed, the plant dies because the short expansion time of its other organs does not allow the excess sugar to be stored elsewhere. The plant dies of being poisoned (personal communication of Guo Yan, CAU, 2006). On the other hand, in sunflowers, where the duration of organ expansion is long, if the terminal cap is removed, the last (normally small) leaves become very large, as well as the stem that bursts under the pressure of excess supply.

5.3.4 Effect of Planting Density on Biomass Partitioning

In tomatoes, as in other cultivated plants (e.g., maize in Ma et al. 2008, see Chap. 11), planting density influences the total weight of the individual plant, but does not influence the partitioning of biomass among the different organ compartments, and therefore the HI remains unaffected (Fig. 5.7).

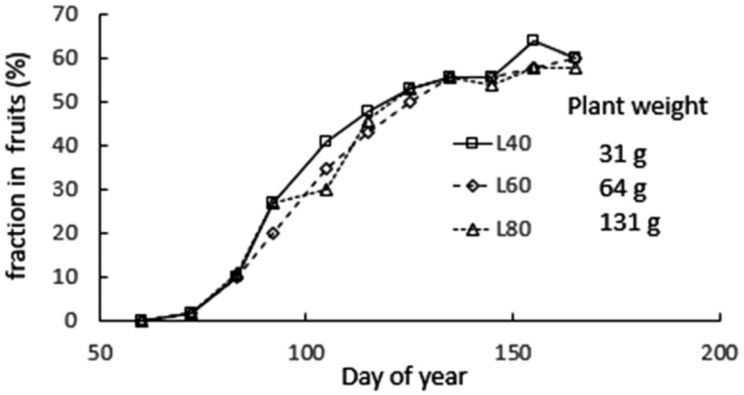

Fig. 5.7 Patterns of the HI during tomato growth at three planting densities: (spacing between plants on a row: $L = 40$ (squares), 60 (diamonds), 80 (triangles) cm). The distance between rows was 80 cm for all three densities. The three profiles corresponding to the three densities are similar, indicating that partitioning is independent of planting density. It should be realized that all trusses were pruned to 7 fruits per truss. On the other hand, the weight of the individual plants is obviously dependent on the density (131, 64, 31 g, respectively). (Ep Heuvelink, Wageningen University)

5.3.5 Effect of the Position of Organs in the Growth

To prove the efficiency of the common pool concept, one experiment was conducted on locating trusses on tomato plants grown with two similar stems for one plant. In the first experiment, every second truss was left for both stems. In the second experiment, all the trusses were left on the first stem, while all the trusses are removed from the second stem. Both experiments have the same number of plants and organs. If the common pool is verified, they must have the same growth, and therefore the same weight per compartment, which is what was observed (Fig. 5.8).

5.3.6 How the Model Works

The TomSim physiological crop model (Heuvelink 1999) is calibrated and validated on many greenhouse experiments. It functions on a daily time step (photosynthesis is calculated at an hourly step).

Once these rules have been defined, and the system parameters have been calibrated, the TomSim model grows the plant population according to the flowchart in Fig. 5.9. The respiration is considered here, but more frequently, only net photosynthesis is considered.

- The plant leaf area is computed from the leaf biomass divided by the thickness (specific leaf weight: SLW); from plant leaf area and planting density, the LAI (leaf area per m^2) can be calculated;

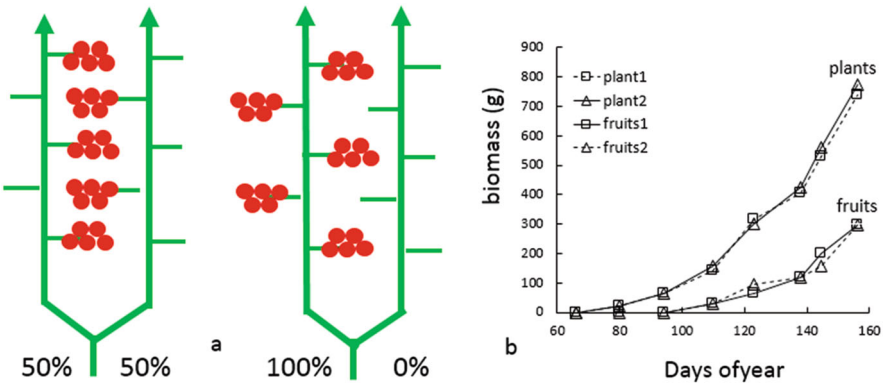

Fig. 5.8 Tomato plants grown with two stems originating from cotyledon axillary buds. (**a**) In 50–50 treatment, on each stem half of the trusses were kept, while in 100–0 treatment, all trusses were kept on one stem and all trusses were removed from the other stem, resulting in plants with the same number of trusses but located differently. (**b**) The two types of plants have the same total plant growth and the same fruit harvest index (HI) (Δ is 50–50 and □ is 100–0), which validates the common pool hypothesis. (Source: Heuvelink 1995)

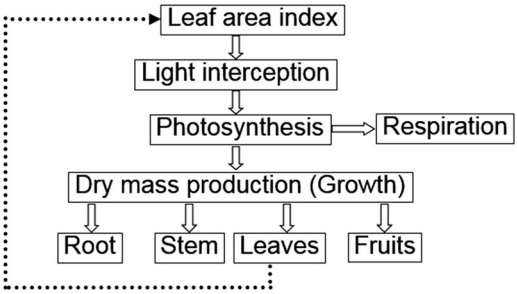

Fig. 5.9 Flowchart of the growth of plant population per m^2 functioning on a daily time step. The biomass that goes to the leaf compartment results in increased leaf area, and hence increased light interception. (Source: Ep Heuvelink, Wageningen University)

- Biomass production depends on LAI, light intensity (PAR), CO_2, and temperature, taking effect in Eq. (5.1);
- The biomass produced can be considered as forming a common pool from which the organs draw for their growth according to their sink strength relative to the total sink strength of all organs together.

Biomass distribution among organ compartments is independent of biomass production. In particular, it does not depend on planting density. It is often stably fractionated according to sink strengths measured directly from the ratio of daily weight increases in vegetative compartments (leaves, stems, and roots) and fruit organs. The leaf compartment provides feedback on the growth.

The TomSim model, which uses the rules validated by the above experiments, gives a good prediction of crop production according to the time of year for all organ compartments (fruits, leaves, stems, and roots) (Fig. 5.10). In greenhouse conditions, the limiting factor is light: the biomass production in the Netherlands is three times less in the winter period than that in the summer period.

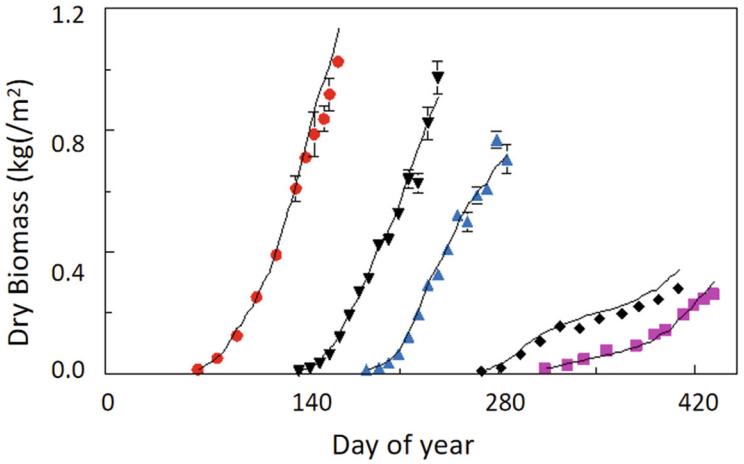

Fig. 5.10 Measured (symbols) and simulated (lines) dry biomass produced per m^2 for a tomato crop planted at different times of the year using the TomSim model. The growth in late autumn (black diamond) and winter (marker □ pink) is strongly slowed down by a lack of light (Heuvelink 1995) (Color figure online)

5.3.7 Review of Physiological Crop Models

Based on simple concepts of biomass production (using eco-physiological factors), and its partitioning in plant compartments, physiological crop models (Marcelis and Gijzen 1998; Marcelis et al. 1998) provide good harvest predictions.

In greenhouses, normally water and temperature are not limiting factors because they can be controlled. The main limiting factor is photosynthetically active light (PAR), which varies greatly over the seasons and is, at best, only 70% transmitted into the greenhouse. The proportionality parameter between the produced biomass and the intercepted light is called *light use efficiency* (LUE). The LUE depends mainly on the CO_2 concentration in the greenhouse and has little dependence on the PAR. For better growth prediction, changes in environmental factors must be incorporated into each simulation step.

In field conditions, the main limiting factors are temperature and water, with sufficient light during the growing season. The use of thermal time compensates for the variation in temperature and makes it possible to linearize the development of the crop according to the sum of daily temperatures. Empirically, the biomass produced per m^2 is proportional to the water transpired by the canopy, which depends on the evapotranspiration value (PET). The proportionality coefficient between the biomass produced and the transpired water is called *water use efficiency* (WUE). The WUE is generally stable. Eq. (5.1) remains valid for computing biomass production per m^2 because the canopy transpiration also depends on the LAI, according to the same formulation as Beer-Lambert's law. When the transpiration is computed, parameter C is no longer the LUE, but the WUE. For example, as an order of magnitude for

plants, 500 L of transpired water per m^2 give about 10 kg of fresh matter or 1 kg of dry matter. In the event of water stress, a water module must be developed that calculates the transpired water as a function of soil moisture and is integrated into Eq. (5.1). The Pilot software (Mailhol et al. 1996) thus predicts the production of different crops according to climatic conditions with rainfall data.

Due to their functioning at the stand and organ compartment level, physiological crop models have several limitations:

- Difficulties in modeling the effect of stresses (water, light, etc.) that lead to organ abortions (meristems, leaves, fruits, branches);
- Difficulties in synchronizing the different modules of the physiological crop model, such as soil moisture model or organogenesis model;
- Lack of information on the position of organs within the crop;
- No consideration of stochastic aspects in the development;
- No consideration of secondary growth;
- Lack of representations (visualizations) of the simulated plants, which is especially relevant for ornamental plants.

5.3.8 *An Example of Functional–Structural Plant Modeling Close to Physiological Crop Models: The GreenLab Model*

Figure 5.11 positions the approach of the GreenLab model in relation to physiological crop models and functional–structural plant (FSPM) models.

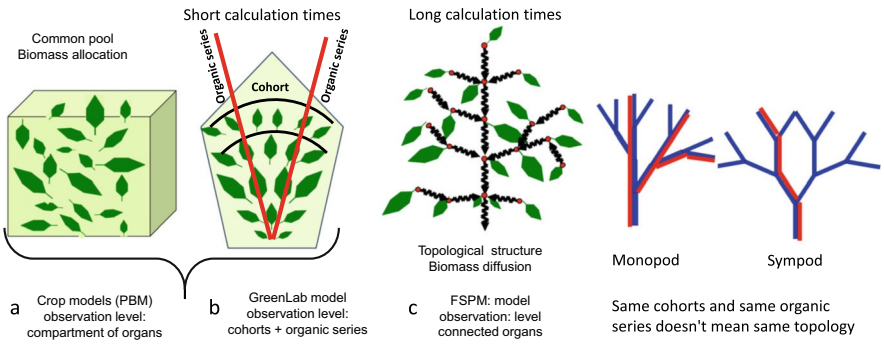

Fig. 5.11 Different approaches to modeling plant growth. (**a**) Physiological crop models gather organs into compartments and use a common pool. (**b**) The GreenLab model uses cohorts and organic series of organs that are orthogonal to each other and also use a common pool. (**c**) Functional–structural plant models (FSPM) use individual organs and source–sink relationships through a topological structure

In most physiological crop models (CM), the organs are grouped into compartments. The number of organs is not of main interest. At each time step of the growth, an allocation of the biomass taken from the common pool goes to the compartment according to a proportion, so the history of the growth is lost if there is no concept of the cohort. The process is not precise, but it is immediate, and simple equations make it work.

In functional–structural plant models (FSPM), each organ is connected to the topological structure. Propagation of the biomass from the source organs takes place in the structure towards the sink organs according to a short time step. The "Common pool" hypothesis can be used or not. Each organ works independently as in a multi-agent system. There is no implicit concept of cohorts. The process is accurate but time-consuming because it requires software to simulate the propagation of biomass within the structure.

GreenLab is a functional–structural plant model, and aims to model plant growth at the phytomer level while remaining compatible with physiological crop models. Plant development is built on the functioning of meristems. A hierarchical and anatomical structure is created. The notion of potential structure also makes it possible to compute the number of organ types per cohort, even in the stochastic case (Chap. 3).

The number of organs produced at each time step is computed by recursive algorithms using a botanical automaton (Chap. 4). These organs are organized into cohorts according to organ type and chronological and physiological ages, with the number of cohorts being a product of them. All organs in a cohort are identical. The development history is preserved, and a strong factorization is carried out, since only one representative organ of each cohort needs to be simulated. At each step of the development, the biomass collected from the common pool goes into the cohorts according to the relative sink strength and the number of organs. The process is based on equations and in the case of Matrix Mode does not require browsing the whole plant structure (as in List Mode), to simulate the biomass partitioning, so it is fast. In GreenLab, the plant is decomposed into spare parts of organs (see below organic series). Thus, organ cohorts provide a functional structure, different and simpler than the anatomical and hierarchical structure, for modeling source-sink interactions. This is characteristic of integrative biology. The construction of the topological structure is optional, and it does not directly participate in the functioning. GreenLab makes it possible to switch from organ-compartment-based functioning (e.g., physiological crop models) to individual-organ-based functioning (e.g., functional–structural models) while maintaining the knowledge acquired from the former.

In the following sections, it is assumed that the climatic conditions are stable and non-stressful to be able to study the model's behaviors under so-called potential growth conditions.

5.4 Plant Demand: The Function of the Development

The plant's demand at a chronological age (CA) t corresponds to the sum of the demands of the active sinks of the growing structure. It is the sum of the products of the numbers of organs (computed by the botanical automaton in the cohorts defined according to their types, physiological and chronological ages) and the values of their sink functions.

5.4.1 Scheme of the Functioning of the Organs

The organs are created by meristems and then expand due to their sink strengths, which allows them to capture biomass from the common pool. The duration of this expansion is measured in growth (or development) cycles (GC or DC). At maturity, the organ sink ceases to compete with others and is no longer part of the plant's demand.

5.4.2 Definition and Form of Sink Functions

The organs can grow over several expansion cycles. The sink strength of an organ of type o with PA φ and expansion duration T_o is modeled, according to its expansion cycle x by the equation:

$$P_o^{\varphi}(x) = p_o^{\varphi} \cdot F_o\left(\frac{x}{T_o}\right) \tag{5.3}$$

where p_o^{φ} is the sink strength of the organ; x is its chronological age (CA); φ is its physiological age (PA); o represents the organ type (a: leaf, i: internode, f: fruit). $F_o\left(\frac{x}{T_o}\right)$ is the variation function of the sink related to its expansion duration. This function is normalized: $\max(F_o) = 1$.

An empirical function is defined in advance, the form of which, controlled by the parameters to be estimated, is flexible enough to adapt to numerical changes in sink values during organ expansion. In GreenLab, this function is a beta law (Fig. 5.12): it shows great plasticity and gives a good prediction of organ expansion. It is defined by two parameters a and b on the interval [0, 1]:

$$\beta(x) = \frac{(a+b-1)! \cdot x^{a-1} \cdot (1-x)^{b-1}}{(a-1)! \cdot (b-1)!} \quad 0 < x < 1 \tag{5.4}$$

This law has the following mean (m) and variance (v) in x [0 1]:

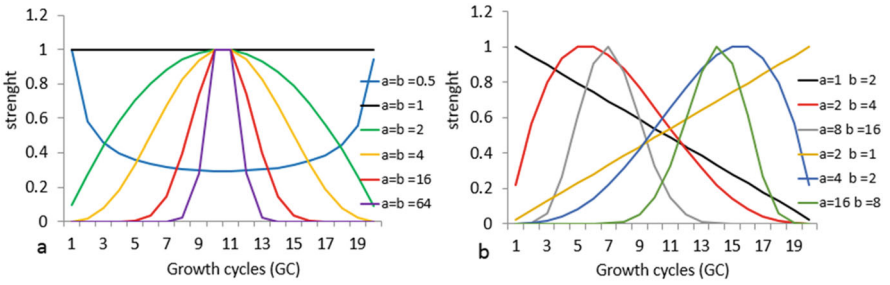

Fig. 5.12 Shapes of sink functions of discretized beta law, normalized over an interval T_o of 20 cycles. (**a**) Symmetrical shape with $a = b$. The values given for a and b are 0.5, 1, 2, 4, 16, and 64. For $a < 1$, the function has a U-shape. For $a = 1$, the function is constant. For $a > 1$, the function has a symmetrical bell shape centered in $m = 10$ ($m = 20a/(a + b)$). The more a and b increase, the less the curve is spread. (**b**) Asymmetrical shape. Examples are given that the pairs of parameters a and b of the beta law are chosen as an example: (1, 2), (2, 4), and (8, 16). The larger $a + b$ is, the less the curve is spread

$$m = \frac{a}{a+b}$$
$$v = \frac{a \cdot b}{(a+b)^2 \cdot (1+a+b)} \tag{5.5}$$

The notations are modified to make the formulation of this equation more appropriate by making it discrete. Note T_o is the domain of x for the CA of the organ expressed in cycles: ($T_o \geq 1$ and $0 \leq x \leq T_o$). The coefficient C_o is calculated so that the maximum of the function is normalized to 1.

We define:

$$F_o\left(\frac{x}{T_o}\right) = C_o \cdot \left(\frac{x+0.5}{T_o}\right)^{a-1} \cdot \left(1 - \frac{x+0.5}{T_o}\right)^{b-1} \cdot \left(\frac{1}{T_o}\right) \tag{5.6}$$

So in the interval [1 T_o], we have the mean:

$$m = \frac{a}{a+b} T_o \tag{5.7}$$

This unimodal function can have various shapes, which may be more or less asymmetrical and spread out. The sink variation function is assumed to be independent of PA. It depends only on its type o. The influence of PA appears only in the multiplicative factor, the sink strength itself. Since sink strengths are relative (see next paragraph), a reference must be set. It is assumed that the sink strength of leaves with PA 1 is equal to the unit: $p_a^1 = 1$.

It is possible to empirically determine the sink function of an organ by monitoring its growth under non-limiting assimilate supply, the so-called potential growth

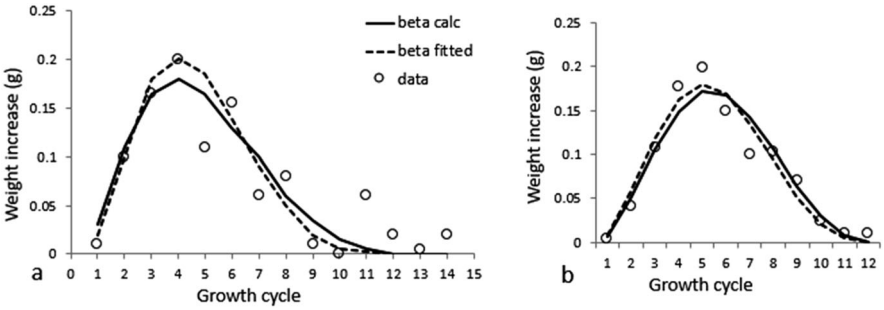

Fig. 5.13 Observed (symbols) increase in weight of a tomato fruit (**a**) and sweet pepper (**b**) as a function of its age measured in cycles (o). The curves represent beta laws. Fitted curves (dotted lines) are close to those calculated from the organs on the stem by inverse method (solid lines) without growth monitoring. (Sources: China Agricultural University (CAU) and Wageningen University)

(Heuvelink 1996b). Establishing the relationship between fruit diameter and fruit weight makes it possible to determine the sink function of fruit without sacrificing it during its growth.

However, the method remains often impractical and applies only to fruits (pepper, tomato). In general, the parameters of the sink functions are called "hidden" parameters. In GreenLab, these parameters are estimated using an inverse method, from measurements on the plant architecture without growth monitoring (Chap. 9). In practice, the expansion time T_o is empirically observed or assessed, and the parameters a and b are estimated from the measurements taken on the architecture.

Figure 5.13 shows an example of the increase in weight of tomato fruit and sweet pepper fruit, measured periodically during their expansion using the allometry between their diameter and weight. The pattern can be described by a beta law. This law is also directly identifiable from the weights of organs scattered on the stem of a plant (without growth monitoring) and whose parameters are identified by the inverse method at the plant level (Chap. 9). The two laws obtained are very similar. This shows the coherence of the model with two different computation methods.

5.4.3 Plant Demand as the Sum of the Sinks of the Organ Cohorts

A botanical study defines the number of organ types per phytomer. From the number of phytomers produced by the botanical automaton, we deduce the numbers of leaves, internodes, and fruits produced in each cycle. The number of phytomers created at each cycle for each PA is computed, either by enumeration during simulating organogenesis in list mode or by calculation using the corresponding development equation in matrix mode. With the latter, we can deduce the number of

organs $N_o^{\varphi}(t)$ produced for a type o at CA t for PA φ. By definition, it constitutes a cohort or set of homologous elements that appeared at the same time. Hence, the expression of the plant's demand at CA t is:

$$D(t) = \sum_{o,\varphi} \left(\sum_{i=1}^{t} N_o^{\varphi}(t-i+1) \cdot P_o^{\varphi}(i) \right) \tag{5.8}$$

where organ type o, of PA φ and aged i cycles have a sink strength $P_o^{\varphi}(i)$ which depends on the maturity i in DC of the organ. They appeared at cycle $t - i + 1$ and are in the number of $N_o^{\varphi}(t-i+1)$. The expression of $D(t)$ is obtained by a convolution that is quick to compute.

5.5 Growth Equations

Same as the development, the growth can be formulated by mathematical equations.

5.5.1 Biomass Partitioning Equations

The expansion by weight of an organ of type o, of PA φ and aged i cycles of development in a plant of CA t (therefore at cycle t) is written:

$$\Delta q_o^{\varphi}(i,t) = P_o^{\varphi}(i) \cdot \frac{Q(t-1)}{D(t)} \cdot \Delta t \tag{5.9}$$

Here $\Delta t = 1$ because the growth cycle is the same with the DC.

Organ expansion depends on the sink strength $P_o^{\varphi}(i)$, the biomass $Q(t-1)$ produced in cycle $t-1$, which is distributed within the plant structure whose total demand is $D(t)$. Note that the sinks in this system are relative because they appear in the numerator and denominator of the expression (Eq. 5.8). It is, therefore, necessary to choose a reference organ. Only the leaves always exist, while in herbaceous plants, the internodes are not measurable at the rosette stage. For this reason, the sink strength of a leaf blade of PA 1 is normalized to 1.

The biomass accumulated in an organ created at i DCs in a plant aged t DC is the sum of expansions:

$$q_o^{\varphi}(i,t) = \sum_{j=i}^{t} P_o^{\varphi}(j-i+1) \cdot \frac{Q(j-1)}{D(j)} \tag{5.10}$$

The weight of organ $q_o^{\varphi}(i,t)$ that appeared at the age $t - i + 1$ is represented $N_o^{\varphi}(t-i+1)$ times in its cohort.

Equation (5.10) can be written in matrix form. A growth operator is defined as one that connects organ biomass to produced biomass and plant demand through the sink functions.

There are as many operators as there are types of organs o, multiplied by the maximum number of PAs ($mx\varphi$). For a tree, there are most often 12 operators (3 types of organs × 4 PAs). The operator's matrix dimension increases as the number of DCs t increases.

$$\begin{bmatrix} q_o^{\varphi}(1,t) \\ q_o^{\varphi}(2,t) \\ \vdots \\ q_o^{\varphi}(t,t) \end{bmatrix} = \begin{bmatrix} P_o^{\varphi}(1) & P_o^{\varphi}(2) & \cdots & P_o^{\varphi}(t) \\ 0 & P_o^{\varphi}(1) & \cdots & P_o^{\varphi}(t-1) \\ 0 & 0 & \ddots & \vdots \\ 0 & 0 & \cdots & P_o^{\varphi}(1) \end{bmatrix} \begin{bmatrix} \dfrac{Q_0}{D_1} \\ \dfrac{Q_1}{D_2} \\ \vdots \\ \dfrac{Q_{t-1}}{D_t} \end{bmatrix} \tag{5.11}$$

This system describes the individual expansion of organs according to their CA of appearance according to their type o, their PA φ, and the evolution of supply on demand: $Q(i-1)/D(i)$. This quotient is equivalent to an internal pressure of the synthesized biomass that must be allocated to the various organs of the botanical structure. It is referred to here as "trophic pressure".

Each organ is a representative of the cohort in which it was born. The number of organs corresponding to rank k is variable: it depends on the number of phytomers produced in the cohort at age k by the botanical automaton. The chronological sequence of organ biomass (left part of the operator in Eq. (5.11)) defines the description of a series of homologous organs along a vegetative axis for their weights.

This series $q_o^{\varphi}(1,t), \ldots, q_o^{\varphi}(t,t)$ is called the "organic series" (Buis and Barthou 1984). It describes the profile of the vegetative axis for the biomass of an organ o positioned according to the rank k of its phytomer.

Since we know the number of organs $N_o(k)$ associated with a rank k, we can also know the total accumulated biomass $SQ_o^{\varphi}(t)$ in the compartment constituted by these physiologically aged organs φ:

$$SQ_o^{\varphi}(t) = \sum_{k=1}^{t} N_o^{\varphi}(k) \cdot q_o^{\varphi}(k,t) \tag{5.12}$$

The sum of all the results $SQ_o^{\varphi}(t)$ for all organs o and PA φ gives at the end the total biomass of the plant.

The plant can be broken down into a small number of categories of axes, which in turn are divided into separate organic series. The description of these series gathers all the necessary information contained from development and growth. This system makes it possible to define very efficient targets for the calibration of the source-sink model from the experimental data (Chaps. 9 and 10). The analysis of the plant

decomposed in separate pieces, such as cohorts or organic series (see below), bypasses the complicated use of the topological structure.

5.5.2 *Considerations on Organic Series*

Buis and Barthou (1984) defined and studied the evolution of an organic series mathematically:

> "All organs of the same morphological nature generated by the same primary meristem during the development of a leafy axis and on which the same morphogenetic character is considered".

For example, this could refer to the weight or surface area of a leaf, the length of the internode, etc. The size of each organ depends on its rank in the series, the CA of the axis and its creation date. The system generates a family of curves that gives the profile of the organic series according to the age of the leafy axis and the dates of creation of the phytomers. Thus, the same types of organs in the same series have different dimensions depending on their rank.

However, the study of Buis and Barthou (1984) remains descriptive because it is based on allometric relationships between the dimensions of the organs that increase according to kinetics based on thermal time and not on source–sink relationships. Nevertheless, the thermal time is often sufficient to follow step by step the development of the axis and the expansion of the organic series generated, as in maize (leaf length, sheaths, internodes) (Fournier and Andrieu 1998).

GreenLab generalizes the notion of organic series, which is no longer necessarily linked to the physical notion of one single axis. The axial notion of organic series, depending on the position of the phytomers on an axis, can be extended to the chronological notion that describes the evolution of the phytomers in successive cohorts. The organic series is "orthogonal" to the notion of cohort in relation to time. The organs can be sorted according to a time step (developmental cycle, DC), which then replaces the notion of rank in the axis. The rank of the series corresponds to the age of the cohort, and the number of representatives of the same organ varies from one cohort to another.

Figure 5.14 shows the same single-stemmed plant at four different growth stages and the evolution and expansion of the resulting organic series.

Time organic series are also defined in monopodial or sympodial structures. In Fig. 5.15, starting from the top of the axes, the same organic series is found identically throughout a plant structure organized according to the principle of the PA. Indeed, the same rank of phytomer from the apex of the living branches and the same PA is characteristic of the same cohort. In the case of monopodial branching (Fig. 5.15a), only the first branch has a complete series, other series are top-down truncated depending on the age at which the branches appear in the structure.

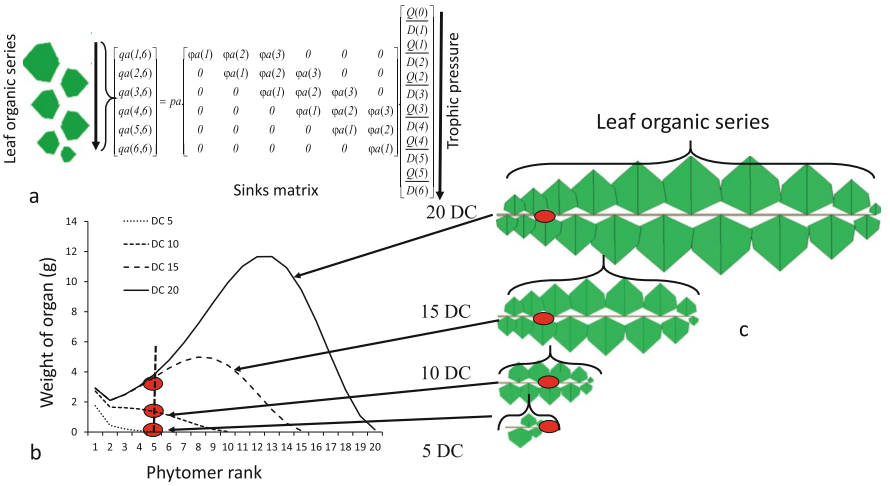

Fig. 5.14 Evolution of the organic series of leaves during a single-stemmed plant growth. This evolution is twofold. On the one hand, we have the development of the series, which increases by adding one phytomer at each cycle, and on the other hand, the individual growth of the organs according to their rank. (**a**) Relationship between organic series and evolution of trophic pressure through the matrix of sinks (with an expansion duration $t_x = 3$ DCs). (**b**) Curves of development and growth of the leaves organic series for periods of 5, 10, 15, 20 DCs. The red dot refers to the rank 5 of the phytomer on the axis whose behavior is particularly examined. On this rank, the expansion of leaf is completed at the age $t_x = 15$ DCs. (**c**) Simulation of the plant for the age of 5, 10, 15, 20 DCs corresponds to the series displayed with the mark of phytomer 5

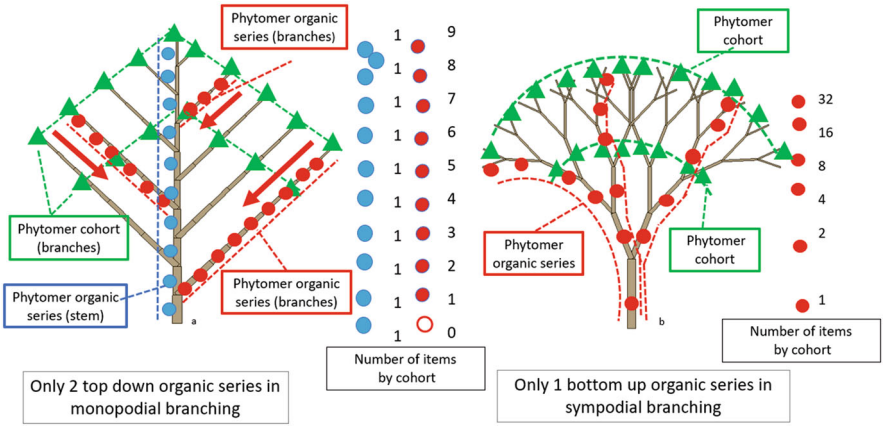

Fig. 5.15 Visualization of organic cohorts and series in plant architecture according to the GreenLab model. (**a**) Case of monopodial branching, (**b**) Case of sympodial branching. The number of organic series depend only on the physiological ages. The phytomers of the same nature and created at the same time form a cohort. The organic series are orthogonal to the cohorts. They can be found in both monopodial and sympodial structures. The same truncated series can be replicated many times in a structure. In this example, there are only two organic series for the monopodial structure: stem and branches, and only one for the sympodial structure

The organic series contains the entire history of source–sink relationships in plant growth. They are effective for data assimilation because they can be found in any architectural model.

5.5.3 Dynamics of Biomass Production of an Individual Plant

5.5.3.1 Production Equation of an Individual Plant

Consider Eq. (5.1) of the production of a stand.

$$Q = C \cdot \mathrm{PAR}(t) \cdot (1 - \exp(-k \cdot \mathrm{LAI}(t))) \cdot \Delta t$$

The reference cultivated area S_c of a crop stand is 1 m^2, which is implicitly included in Eq. (5.1). It is made explicit in Eq. (5.13); the LAI is written as Sf/S_c; S_f is the leaf surface of the canopy and S_c is the surface area of the stand on the ground:

$$Q = C \cdot \mathrm{PAR} \cdot S_c \cdot \left(1 - \exp\left(-k \cdot \frac{Sf}{S_c}\right)\right) \cdot \Delta t \tag{5.13}$$

To link the growth to the development for an individual plant, the expression must be expressed in DC, measured in thermal time. During the DC t, the light energy received by the canopy is denoted as PAR(t) and the leaf area of the canopy is assumed to stay constant during one DC and is denoted as $Sf(t)$.

This equation can be adapted to an individual plant.

$$Q(t) = C \cdot E(t) \cdot Sp(t) \cdot \left(1 - \exp\left(-k \cdot \frac{Sf(t)}{Sp(t)}\right)\right) \tag{5.14}$$

where $E(t)$ is the growth factor (light (PAR) or transpired water (PET) as appropriate) and C is the resource use efficiency (water use efficiency or light use efficiency, respectively). They are supposed to be known.

The leaf area and weight of a plant can be measured for each DC by sampling from the population. In cycle t, we can, therefore, know the increase in biomass $Q(t)$ of the individual plant produced by its leaf area $Sf(t)$. On the other hand, S_c, which is the surface area of the stand, is not defined a priori for an individual plant. Let $Sp(t)$ be this unknown value assigned to the individual plant in the cycle t. It can be estimated by solving Eq. (5.14) at each DC, i.e., by assuming the changes in known $Q(t)$ and $Sf(t)$ and looking for the values of $Sp(t)$ that give equality to each cycle.

$Sp(t)$ becomes the production surface of the plant (that is the computed surface area occupied by the plant on the ground in the stand), defined as the "solution" of Eq. (5.14) in the cycle t. It is the effective production surface that intercepts light, considering the overlapping of the leaves and its spreading on the ground. The ratio

$\frac{Sf(t)}{Sp(t)}$ is an optimized individual *LAI*. However, this requires some comments.

The expression $S\varphi(t) = Sp(t) \cdot \left(1 - exp\left(-k \cdot \frac{Sf(t)}{Sp(t)}\right)\right)$ measures the surface of the shadow on the ground projected by the foliage, which quantifies the light intercepted with the sun at its zenith; it is call the photosynthetic surface.

$Sp(t)$ is first a calibration parameter. While Beer-Lambert's law may not be applicable if the foliage is heterogeneous, the production area is always a solution of Eq. (5.14). If the area of interception of light by the foliage is the total leaf area (leaves do not overlap), $Sp(t)$ takes on an infinite value and loses its topographical significance. This situation concerns the juvenile stage of the plant, where all the leaves are illuminated. It corresponds to a limited Taylor series development of Eq. (5.14) at order 1. Biomass increases become proportional to the leaf area. Eq. (5.14) is then approximated as:

$$Q(t) \approx C \cdot k \cdot E(t) \cdot Sf(t) \tag{5.15}$$

A priori, the production area of the plant $Sp(t)$ varies with each cycle in Eq. (5.14). Due to a high planting density d per unit area of stand S_c, when competition between plants makes them touch each other and limits the expansion of the projection of foliage on the ground to an average individual area Sd ($Sd = S_c/d$), then $Sp(t)$ should stabilize around $Sp(t) \approx Sd$.

Indeed, if the expression $k \cdot \frac{Sf(t)}{Sp(t)}$ is greater than 3, the term $\exp\left(-k \cdot \frac{Sf(t)}{Sp(t)}\right)$ is negligible and Eq. (5.14) is written as:

$$Q(t) \approx C \cdot E(t) \cdot Sp(t); Q(t) \approx C \cdot E(t) \cdot Sd \tag{5.16}$$

At the start of plant growth, leaves do not overlap, $Sp(t)$ is very large and is not involved in biomass production (Eq. 5.14). When the plants come into contact, $Sp(t)$ takes the fixed value Sd. Sd becomes an approximate solution of Eq. (5.14). The individual production area is the area of ground occupation by the plant, which is equivalent to the projected surface of the foliage and can be written as $Sp \approx Sd$. In the case of high planting density, neighboring plants touch each other soon, as if Sp was constant.

The equivalence $Sp \approx Sd$ in GreenLab has been verified and validated for various field crops (tomato, maize, beet, Sect. 5.8.2.1) and for various planting densities (Chaps. 9 and 10). The role of Sp is discussed in more detail below.

In order to study the behavior of GreenLab during the growth, it is assumed that the parameters $E(t)$ and the production area $Sp(t)$ per cycle are constant. They are represented by E and Sp, respectively. We choose $E = 1$ and Sp as the solution of Eq. (5.14). $r = 1/C$ is defined as a calibration coefficient.

5.5.3.2 Leaf Surface Expression

The functioning time of the leaves (in cycles) is indicated by the parameter t_a. Let us consider it here equal to the duration of their expansion, denoted as t_x. In order to calculate the leaf area of the plant, it is necessary to sum the masses of the functional leaves and divide by their thickness ε, which is assumed to be constant. The functional leaf area $Sf(t)$ can be computed by Eq. (5.17), where the index φ refers to the PA (ranging from 1 to $mx\varphi$). Within a cohort of leaves that appeared at CA i, the number of leaves $N_a^{\varphi}(i)$ and their individual biomass are recorded. Two cases must be distinguished for the computation of the area according to whether the age of the plant t on DC exceeds the lifespan of the leaves t_a or not. Indeed, one case $t < t_a$ corresponds to the beginning of the plant's growth, as long as no leaves have died yet. On the other hand, in the other case $t \geq t_a$, only leaves whose CA is less than $t - t_a + 1$ are still functional. A unique equation can describe these two cases, the distinction being represented by the limits of the index of the second sum in the expression below. The leaf area is computed as:

$$Sf(t) = \frac{1}{\varepsilon} \cdot \sum_{\varphi=1}^{mx\varphi} \sum_{i=\max(1,\ t-t_a+1)}^{t} N_a^{\varphi}(i) \cdot q_a^{\varphi}(i,t) \tag{5.17}$$

5.5.3.3 Dynamic Growth Equation

By expressing the leaf surfaces as a function of the previous Q/D ratios (Eq. 5.17), we obtain the generic recurrence Eq. (5.18) that characterizes the increase in biomass $Q(t)$ at cycle t of a computational plant according to GreenLab:

$$Q(t) = \frac{E \cdot Sp}{r} \cdot \left(1 - \exp\left(-\frac{k}{\varepsilon \cdot Sp} \cdot \sum_{i=\max(1,\, t-t_a+1)}^{t} \sum_{\varphi=1}^{mx\varphi} N_a^{\varphi}(i) \cdot \sum_{j=i}^{t} \frac{P_a^{\varphi}(j-i+1) \cdot Q(j-1)}{D(j)}\right)\right) \tag{5.18}$$

In real plants, the weights of the plant and its compartments are measurable; their simulated values can be computed from the sum of the increase in biomass per cycle.

5.5.4 How Recurrence Works During the Growth

Consider a simplified plant with only one PA, without secondary growth or root system and without fruit. The number of leaves per phytomer is 1. The functioning time of the leaves is t_a and the expansion time of the organs (leaves and internodes) t_x

equals to t_a. The sink functions of the leaves and internodes are, respectively, $P_a(t)$ and $P_e(t)$. The seed biomass is Q_0.

5.5.4.1 Production and Allocation of Biomass during the First Cycle

- Computation of the demand:

There is only one phytomer created from the seed. The number of leaves produced is therefore $N_a(1) = 1$ (case of monocotyledonous plant) and the number of internodes $N_e(1) = 1$. The demand for the first cycle is, therefore:

$$D(1) = N_a(1) \cdot P_a(1) + N_e(1) \cdot P_e \tag{5.19}$$

- Biomass and leaf construction:

The amount of biomass taken by a leaf $q_a(1, 1)$ in the first cycle can be computed, the demand of the plant being $D(1)$ and the volume of biomass given up by the seed being Q_0. The notation $q_o(i, j)$ refers to the mass at the cycle j of the organ o (a for leaves, e for internodes) that appeared at the cycle i.

$$q_a(1, 1) = \frac{P_a(1)Q_0}{D_1} \tag{5.20}$$

The surface of the leaf is written as (Sect. 5.3.2):

$$Sf(1) = \frac{q_a(1, 1)}{\varepsilon} \tag{5.21}$$

- Internode construction:

The amount of biomass from the seed that goes to the internode equals to:

$$q_e(1, 1) = \frac{P_e(1)Q_0}{D_1} \tag{5.22}$$

The allometric relationships (Sect. 2.3.2) are used to obtain the shape:
The length of the internode:

$$h_{1,1} = \sqrt{b_e}(q_e(1, 1))^{\frac{1+\gamma}{2}} \tag{5.23}$$

and the surface of its section:

$$s_{1,1} = \sqrt{\frac{1}{b_e}} (q_e(1,1))^{\frac{1-\gamma}{2}} \tag{5.24}$$

- Computing the biomass production:

Once the surface of the leaf has been established, the biomass production can be computed by Eq. (5.14):

$$Q(1) = \frac{E \cdot Sp}{r} \cdot \left(1 - \exp\left(-k \frac{Sf(1)}{Sp}\right)\right) \tag{5.25}$$

5.5.4.2 Generalization by Recurrence to Cycle *T*

It is assumed that the recurrence equation is validated until the cycle $t - 1$.

- Computation of the Demand:

The numbers of leaves and internodes produced in the cycle t by the botanical automaton of the architectural model are, respectively, $N_a(t)$ and $N_e(t)$. The CA of the organs can potentially be up to t cycles for organs that appeared in the first cycle: the sum of the cohort sinks must, therefore, be between 1 and t. Eq. (5.8) gives:

$$D(t) = \left(\sum_{i=1}^{t} (N_a(t-i+1) \cdot P_a(i) + N_e(t-i+1) \cdot P_e(i))\right) \tag{5.26}$$

The terms of this sum correspond to the demand of the organs of age i in DC (sink functions $P_o(i)$), which are in number $N_o(t - i + 1)$ as they appeared in the cycle $t - i + 1$.

- Leaf construction.

We move from cycle t—1 to cycle t by increasing the size of Eq. (5.11) of one unit, which gives the volume of a single leaf per cohort using leaf sink function $P_a(i)$:

$$\begin{bmatrix} q_a(1,t) \\ q_a(2,t) \\ \vdots \\ q_a(t,t) \end{bmatrix} = \begin{bmatrix} P_a(1) & P_a(2) & \cdots & P_a(t) \\ 0 & P_a(1) & \cdots & P_a(t-1) \\ 0 & 0 & \ddots & \vdots \\ 0 & 0 & \cdots & P_a(1) \end{bmatrix} \begin{bmatrix} \frac{Q_0}{D_1} \\ \frac{Q_1}{D_2} \\ \vdots \\ \frac{Q_{t-1}}{D_t} \end{bmatrix} \tag{5.27}$$

The left vector represents the organic time series of leaf weights.
The surface *Sfa* of a leaf of the cohort that appeared in the cycle i is written as:

$$Sfa(i,t) = \frac{1}{\varepsilon} q_a(i,t) \tag{5.28}$$

The leaf surface of the plant is written as:

$$Sf(t) = \frac{1}{\varepsilon} \sum_{i=\max(1,\ t-t_a+1)}^{t} N_a(i) \cdot q_a(i,t) \tag{5.29}$$

- Building of the internodes of the t^{th} cycle.

  We have the volume of the internodes by Eq. (5.10) using leaf sink function $P_e(i)$:

$$\begin{bmatrix} q_e(1,t) \\ q_e(2,t) \\ \vdots \\ q_e(t,t) \end{bmatrix} = \begin{bmatrix} P_e(1) & P_e(2) & \cdots & P_e(t) \\ 0 & P_e(1) & \cdots & P_e(t-1) \\ 0 & 0 & \ddots & \vdots \\ 0 & 0 & \cdots & P_e(1) \end{bmatrix} \begin{bmatrix} \frac{Q_0}{D_1} \\ \frac{Q_1}{D_2} \\ \vdots \\ \frac{Q_{t-1}}{D_t} \end{bmatrix} \tag{5.30}$$

  The left vector represents the organic time series of internodes weights. Allometries give the lengths and surfaces of the sections of the internode. Length from the internode i to the cycle t:

$$h_{i,t} = \sqrt{b_e} (q_e(i,t))^{\frac{1+\gamma}{2}} \tag{5.31}$$

  Surface of the section from the internode i to the cycle t:

$$s_{i,t} = \sqrt{\frac{1}{b_e}} (q_e(i,t))^{\frac{1-\gamma}{2}} \tag{5.32}$$

- Biomass production at the cycle t.

  Biomass production at the cycle t is given by Eq. (5.14):

$$Q(t) = \frac{E \cdot Sp}{r} \cdot \left(1 - \exp\left(-k \frac{Sf(t)}{Sp}\right)\right)$$

Recurrence works and the plant, therefore, grows from cycle to cycle by increasing the size of the growth equation by one unit at each CA and by alternating the feedback between plant development (organ creation) and the production and distribution of biomass that ensures their expansion.

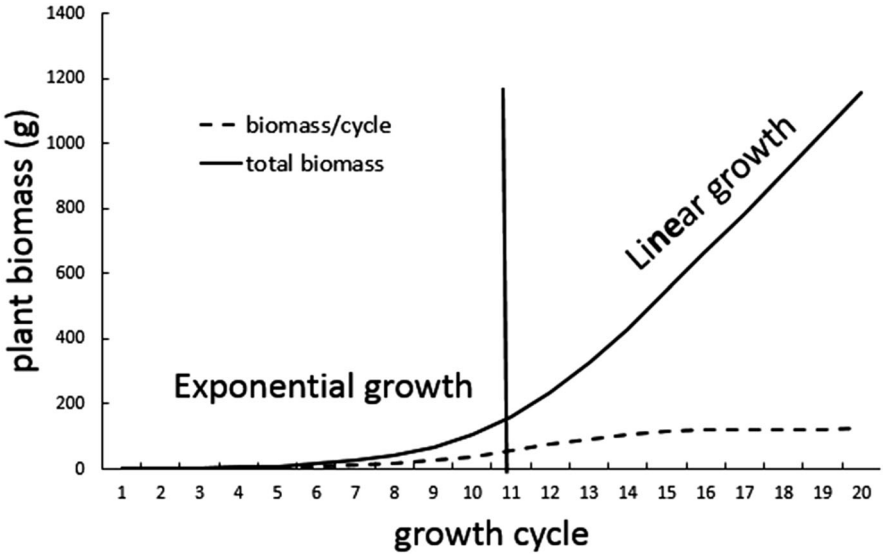

Fig. 5.16 Biomass production per cycle (dashed line) and cumulative weight (solid line) during the growth of a computational plant according to GreenLab (Eq. 5.14) in the case of high planting density (*Sp*). Initially, the growth is exponential (Eq. 5.15) and smoothly becomes linear (Eq. 5.16), because of the effect of the density

5.5.5 How the GreenLab Model Works

GreenLab at the individual plant level works similarly to the TomSim model at the stand level. According to Eq. (5.14), under normal conditions, the biomass produced at each cycle at the beginning of growth grows exponentially. Then, when the limiting effect of the production area *Sp* is reached, the biomass produced at each cycle becomes constant. Correlatively, the weight of the plant, i.e., the sum of $Q(t)$, increases exponentially at the beginning of the growth and then linearly with time under the effect of the limitation due to *Sp* (Fig. 5.16), as long as the senescence of the leaves does not decrease the LAI. This is well verified in cultivated plants, including beetroot (Lemaire et al. 2008; Lemaire 2010) (Fig. 5.30).

GreenLab is available at the organ level. A physiological crop model at the compartment level can be considered as a "projection" of GreenLab at the compartment level, where the sum of the organs reconstructs the compartments. Once these are reconstituted, GreenLab gives the same behavior as physiological crop models (Tomsim, Pilote) for the compartments (leaf indices, harvest indices, etc.). But GreenLab runs at a finer spatial scale, because it simulates, from the seed, the development and growth of the plant structure at the level of the phytomer, which makes it possible to rebuild the plant architecture. Figure 5.17 is thus an extension of Fig. 5.9.

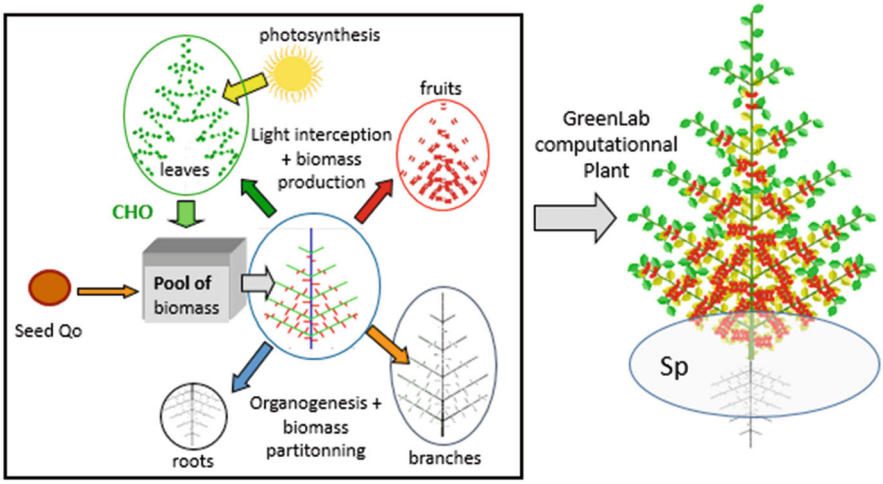

Fig. 5.17 Flowchart of the functioning of GreenLab

5.6 Behavior of the Model: Case of Free Growth

The mathematical study of the model's behavior is an important step in its construction. It makes it possible to establish the influence of the parameters on the growth of the plant. The model equations make it possible to validate the performance of the computer program that numerically simulates the growth and architecture of the plant without explicitly incorporating these equations.

Free growth refers to the case where biomass production is proportional to leaf area, which occurs at the beginning of a plant's growth when the leaves do not yet overlap (Eq. 5.15). The production surface *Sp* is not involved.

Equation (5.14) can be studied in simplified cases. At first, we consider plants with phytomers consisting of an internode with one or more leaves, possibly several fruits and axillary meristems. There is no root system and no secondary growth. Only one PA is also considered. The sinks of the leaf organs and internodes are constant and have the same expansion time t_x equal to the functioning time t_a of the leaves.

By Taylor development limited to the first order, the simplified Eq. (5.18) with a single PA becomes:

$$Q(t) = \frac{E}{\varepsilon \cdot r} \cdot \sum_{i=\max(1,\, t-t_a+1)}^{t} N_a(i) \cdot \sum_{j=i}^{t} \frac{P_a \cdot Q(j-1)}{D(j)} \tag{5.33}$$

The demand of the plant is the sum of the sinks of the organs that compose it. By designating the number of leaves (n_a), internodes ($n_i = 1$) and fruits (n_f), and their sink strengths P_a ($P_a = 1$), P_e and P_f, respectively, the sink strength of the phytomer P_p is written as:

$$P_p = n_a \cdot P_a + P_e + n_f \cdot P_f \tag{5.34}$$

where n_a is the number of leaves per plant ($n_a = 1, 2, \ldots$) and $N_p(i)$ is the number of phytomers with active leaves in the cycle i. Hence, the number of leaves:

$$N_a(i) = n_a \cdot N_p(i) \tag{5.35}$$

It is assumed here to simplify that all organs have the same duration of expansion t_x.

The demand equation is written as:

$$D(i) = \sum_{j=1}^{i} N_p(j) \cdot P_p \tag{5.36}$$

Let us assume hereafter:

$$A = r \cdot \varepsilon \cdot P_p \tag{5.37}$$

The coefficient A includes the action of three parameters on the growth ($1/r$ is resource use efficiency, and ε is the thickness of the leaf). Parameter E represents the energy supplied to the plant by the environment during each DC, which here is assumed to be constant and normalized with $E = 1$.

Equation (5.33) is simplified with this notation:

$$Q(t) = \frac{n_a \cdot E}{A} \cdot \left(\sum_{i=\max(1,\ t-t_a+1)}^{t} Q(i-1) \right) \tag{5.38}$$

This recurrence equation is effective in studying the behavior of the model. To make it simple, we fix $n_a = 1$ (one leaf per phytomer). Two cases can be distinguished.

5.6.1 Conditions for Exponential Growth for $\mathbf{T < t_a}$

When $t < t_a$, all leaves are functional since the age of the plant is less than the duration of their functioning.

For $t_a = 1$ (leaf function and expansion only last one cycle), Eq. (5.38) becomes:

$$Q(t) = \left(\frac{E}{A}\right)^t \cdot Q_0 \tag{5.39}$$

And for $t_a > 1$

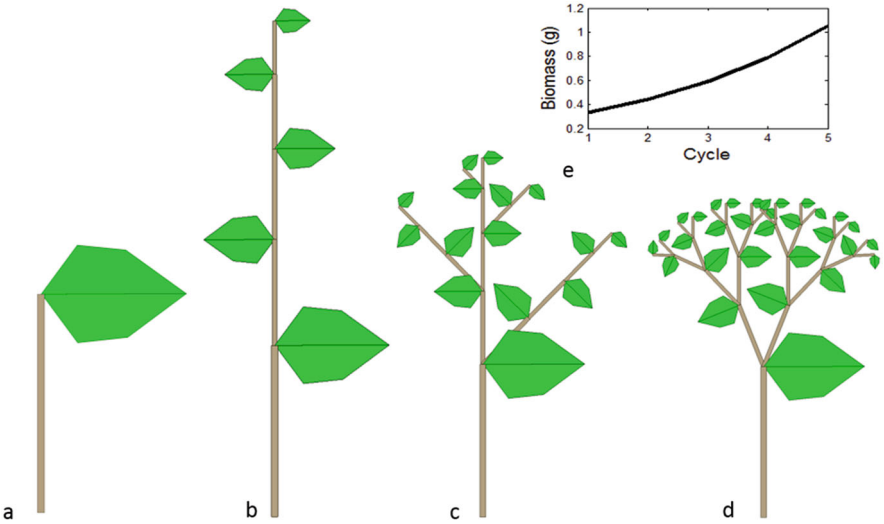

Fig. 5.18 Growth of architectural models with all organs expanding. Plant (**a**) has only one growing phytomer and therefore no development. Plants (**b**, **c**, **d**) follow the developments of a single-stemmed, branched monopodial, and branched sympodial plant, respectively, (**e**), the four plants produce the same total biomass and leaf area with exponential growth

$$Q(t) = \frac{E}{A} \cdot \left(1 + \frac{E}{A}\right)^{t-1} \cdot Q_0 \tag{5.40}$$

These equations explain the exponential growth pattern generally observed in the juvenile growth stage of a plant until the age limit for leaf function is reached. Moreover, the number of phytomers is not involved in the final equation, which means that the development has no influence on the growth. It means that whatever their architectural model, plants with the same functional parameters will have the same trajectory of biomass production. The sum of the weights of the phytomers is independent of the architectural model. Therefore, the more phytomers there are, the smaller their weights are (Fig. 5.18).

For $t_a = 1$, there can be a meta-stable equilibrium if $E/A = 1$.

But if $t_a > 1$, the growth is necessarily exponential according to Eq. (5.40).

In Fig. 5.18, the organs have constant sinks equal to 1, t_a and t_x are 5 DCs. The demand of the plant **a** is $D(5) = 2$, that of the plant **b** is $D(5) = 2 \times 5$, that of the plant **c** is $D(5) = 2 \times (5 + 10)$, and that of the plant **d** is $D(5) = 2^{5-1}$.

These four plants produce the same biomass, and they have the same growth in terms of plant compartments, but different development and, therefore, different architectures. However, in a physiological crop model, these differences are not distinguished.

5.6.1.1 Seed Effect on the Growth

5.6.1.1.1 Influence of the Seed on Plant Growth

We notice in Eqs. (5.39 and 5.40) the importance of Q_0, which is the amount of biomass provided by the seed at the origin of the growth. The plant biomass is proportional to the seed biomass at the beginning of the growth as long as $t \leq t_a$. This is well verified in reality.

In 1920, Professor Achille Urbain, Director of the French Museum (1942–1949), in his thesis on botany (Urbain 1920), carried out experiments to remove albumen of cotyledons to a greater or lesser extent depending on the nature of the seed on various species. He compared the development and growth of the resulting plants with a control plot. The removal of seed reserves significantly reduces both development and growth. The plants obtained were dwarf plants because they produced fewer phytomers, and the organs were atrophied (Fig. 5.19).

More recently, we have observed the germination of cocoa seedlings after weighing the seeds at the beginning. Figure 5.20a shows the effect of the seed on the beginning of growth on a young cocoa tree.

It may not be sufficient to assign a single cycle of seed biomass distribution from seed to seedling, especially in the case of big seeds, such as avocado or coconut. In this case, the seed gradually empties itself over several cycles according to a specific pattern. If we assume an exponential decrease, the quantity released to cycle t is $Q_{\text{seed}}(t) = Q_0 \cdot c^t$. The parameter c is the biomass rate released by the seed at each cycle. In the general case, the photosynthesis will gradually take over (Fig. 5.20b and solid line in Fig. 5.20d). In the absence of photosynthesis, the biomass available per cycle tends to zero (Fig. 5.20c and dotted line in Fig. 5.20d).

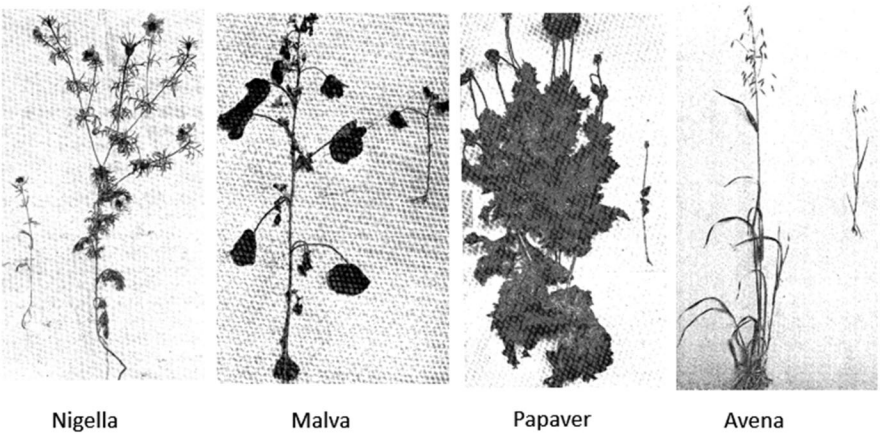

Fig. 5.19 Effect of removing a large part of the albumen from seeds on plant development and growth by Achille Urbain (1920). This means drastically reducing the reserves for germination. We get dwarf plants. On the photographs of four plant species (Nigella, Malva, Papaver, Avena), we can compare the controls with the ex-albuminated plants

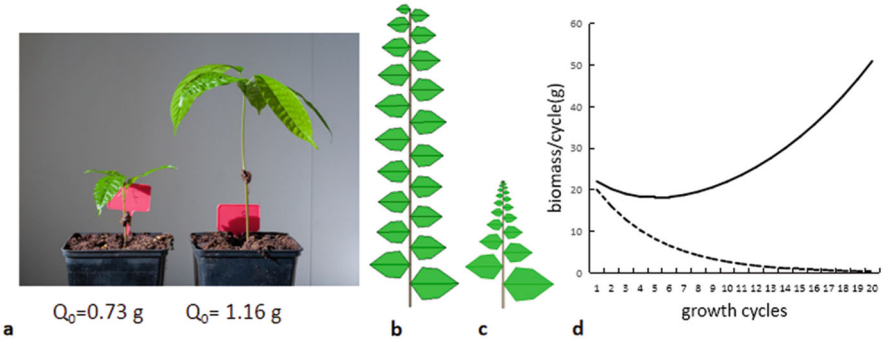

Fig. 5.20 (**a**) Effect of seed weight on seedling size. (**b**, **c**, **d**) Simulation of the effect of seed emptying in several cycles, with photosynthesis relay (**b** and solid line in **d**) or without relay (**c** and dotted line in **d**)

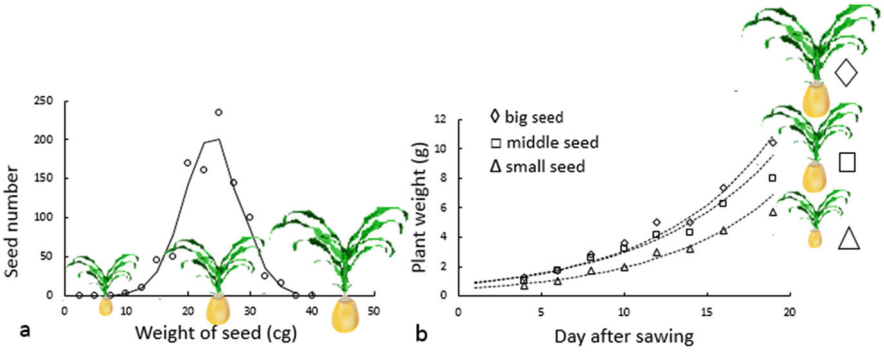

Fig. 5.21 Effect of seed size on the growth of seedlings on maize. (**a**) The weight of seeds has a normal distribution. (**b**) Seedling growth is verified as exponential (free growth, Source Ma Yun-Tao, China Agricultural University (CAU))

5.6.1.1.2 Influence of Seed Weight on Maize Growth at Early Stage

The quantitative effect of the seed on maize growth was specified by Ma Yun-Tao (personal communication, CAU, 2006). From a batch of 950 seeds of the same variety, seed weights varied between 0.15 and 0.35 g (Fig. 5.21a). The seed weights were distributed according to a normal distribution ($\mu = 0.24$ g, and $\sigma = 0.045$ g).

Three weight batches of seeds are made up: big seeds 0.32–0.34 g, medium seeds 0.24–0.26 g, and small ones 0.1–0.18 g, the germination of which is monitored over a period of 20 days.

At this stage, the seedlings have developed five leaves. The increase in biomass of seedlings is measured every two days (Fig. 5.21b). The seedling weight grows exponentially, as predicted by the model for free growth (Eq. 5.15). The weights of the small seeds $Q_s(j)$ and the big seeds $Q_b(j)$ observed are adjusted according to

the number of days d after germination using the equation $Q(i) = a \cdot \exp(b \cdot i)$. The coefficients a and b are calculated by regression.

$$Q_s(i) = 0.48 \cdot \exp(0.14 \cdot i); \quad Q_b(i) = 0.76 \cdot \exp(0.14 \cdot i).$$

It can be seen that the coefficients b are the same, so the ratio of seedling weights during the growth is constant. In addition, the weight of a seedling is an increasing function of the measured seed weight.

The model is well verified here in this simple experimental case.

5.6.1.1.3 Influence of Seed Weight on Germination of Pterocarpus Tree

In Ivory Coast, Adji Beda studied the effect of seed size on germination of Pterocarpus tree. Figure 5.22 shows the appearance of the seeds and their weight distribution. This distribution tends to a normal distribution as for maize.

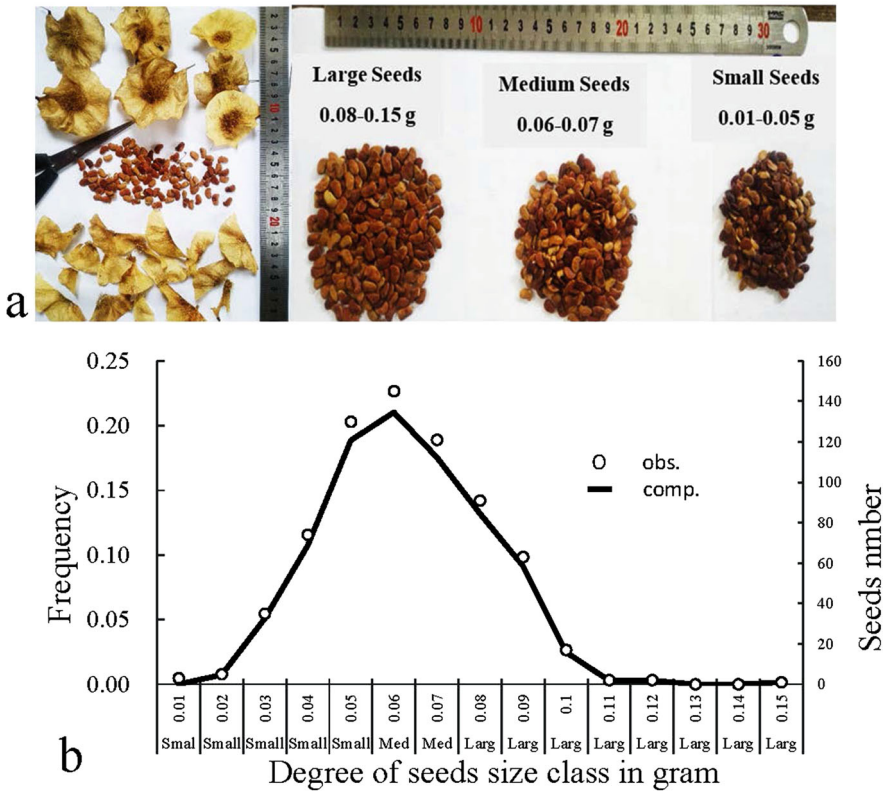

Fig. 5.22 Photos and distribution of seed size of Pterocarpus: (**a**) Photos of seeds. (**b**) Sorting seeds into large, medium, and small categories from left to right and distribution of seeds number and frequency according to their size

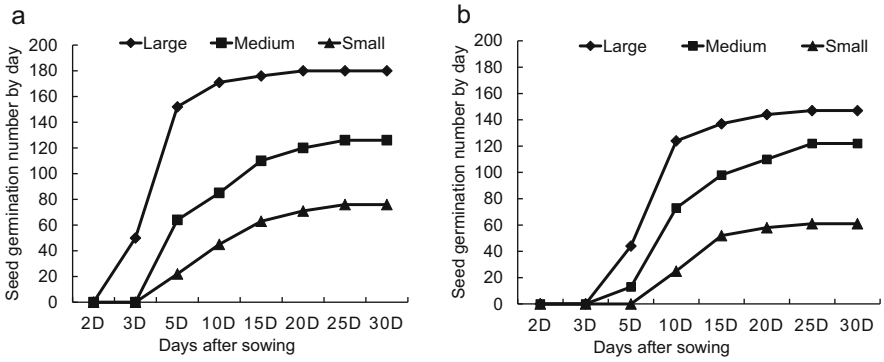

Fig. 5.23 Germination dynamics of three sizes of seeds of *Pterocarpus* tree at Daloa (**a**) and Korhogo (**b**)

Fig. 5.24 Influence of seed reserves (large, medium, small) on seedling size and influence of the station environment (stress) on seedling size at the stations of Daloa (**a**) and Korhogo (**b**)

The following of the germination rates as a function of time shows that they increase with the volume of the seed (Fig. 5.23). This generates a heterogeneity in the seed dormancy and thus in the development of the seedlings at the stand level. Here two stations are represented: Daloa and Korhogo. At the Daloa station, seeds with large size get 100% of germination, while small seeds have less than 50% germination. At the Korhogo station, only 88% of the seeds germinate due to water stress, which is reflected in the germination rates.

The size of the young seedling is directly proportional to the seed reserve, as observed in cocoa tree (Fig. 5.24). Moreover, the same seed batch gives seedlings of different sizes depending on the environmental stress (climate, soil) of a station. Thus, in Korhogo the seedlings are smaller than those in Daloa.

In conclusion, from a modeling point of view, it is essential to integrate the effect of seed reserves (Q_0) to initiate the growth correctly. This aspect is absent in physiological crop models. The seed effect generates heterogeneity in the stand at two levels. The first is the variation of the seed size which modifies plant growth

within the stand, the second is the variation of the dormancy ending which modifies plant development within the stand (see maize section in Chap. 11). However, the seed effect disappears progressively with the effect of planting density.

5.6.1.2 Influence of the Removal of Axillary Meristems

At the juvenile stage, the model predicts that growth does not depend on the architecture. Therefore, if axillary meristems are removed from a branched plant at birth, the resulting single-stemmed plant should weigh the same as the branched control plant. This fact is verified experimentally on plants such as coffee trees in the young stage. Removal of axillary meristems during the growth results in an increase in the volume of organs of the stem to an equivalent biomass of the whole unpruned plant (Fig. 5.25). Removing meristems reduces the demand and therefore increases the volume of the remaining organs. Similar experiments on other species, such as Cotton, give the same type of behavior.

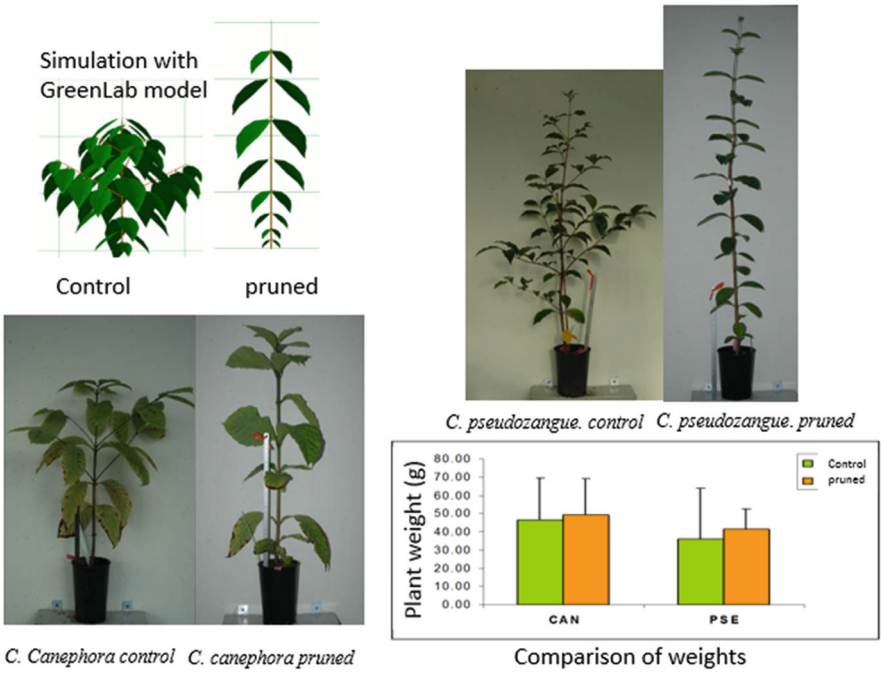

Fig. 5.25 Coffee trees with branches (control) and pruned in free growth [S. Sabatier, AMAP]. All leaves are functional for these plants at early stage. The production is proportional to the leaf area. Axillary meristems have been removed for pruned coffee trees. In accordance with the simulated prediction of GreenLab, pruned coffee trees have larger phytomers, but keep the same total weight as that of the control coffee trees

5.6.2 *Condition for Steady Growth, where* $\mathbf{T > t_a}$ *and* $\mathbf{t_a \geq t_x}$

In this case, the growth time of the plant exceeds the functioning time of the leaves, which wither and no longer participate in the functioning at the end of t_a cycles after their creation. It is assumed here that the functioning time of the leaves t_a is equal to or greater than the expansion time of the organs t_x: $t_a \geq t_x$. Moreover, to simplify, it is assumed that the sinks are constant and equal to 1, thus the phytomer has only one leaf and no fruit.

Let us consider the conditions required for the growth to stabilize. It is sufficient that demand D is limited and that the Q/D ratio (the trophic pressure) tends towards a limit. For the demand to be limited, the life of the axes must be limited. After a while, the newly created phytomers exactly replace the old ones belonging to dead axes. Starting from the growth Eq. (5.33), in order to achieve an equilibrium, the following results are established in different cases:

- If $t_a = 1$ and $t_x = 1$.

  We have the production from Eq. (5.39):

$$Q(t) = \left(\frac{E}{A}\right)^t \cdot Q_0.$$

  Growth is steady only for $E/A = 1$. In this case, the production $Q(t)$ is constant and is equal to Q_0. Otherwise, the growth becomes exponential (increasing or decreasing).

- If $t_a > 1$ and $t_x = 1$.

The leaves work several cycles, but the expansion of the organs only lasts one cycle. As long as $t \leq t_a$, the production is written from Eq. (5.40):

$$Q(t) = \frac{E}{A} \cdot \left(1 + \frac{E}{A}\right)^{t-1} \cdot Q_0$$

When $t > t_a$, the leaves stop working after t_a cycles. The growth will stabilize for each cycle if: $\frac{E}{A} = \frac{1}{t_a}$. After the number of t_a DCs, the production will then tend towards the limit value:

$$Q_l = \frac{2 \cdot Q_0}{1 + t_a} \tag{5.41}$$

- If $t_a > 1$ and $t_a = t_x$,

As long as $t \leq t_a$, the production is exponential and is given by Eq. (5.40). The growth will stabilize beyond $t > t_a$ if the following equality is verified:

$$\frac{t_a + 1}{2} \cdot \frac{E}{A} = 1 \tag{5.42}$$

The production limit Q_l is found by iteration on Eq. (5.38).

- If $t_a > 1$ and $t_a \geq t_x$, this is the general case.

As long as t $\leq t_a$, the production is exponential and is given by Eq. (5.40). The growth stabilizes for $t > t_a$ if the following equality is verified:

$$E \cdot \frac{1}{A} \cdot \left(\frac{t_x + 1}{2} + t_a - t_x\right) = 1 \tag{5.43}$$

This production limit Q_l is also found by iterations on Eq. (5.38).

In summary, the equilibrium equations of the production depend on the functioning time t_a and the expansion time t_x of the organs, a structural coefficient A and the climatic factor E. The growth is, therefore, stabilized in free growth whatever the architectural model if the demand is limited and if the condition of equality given by Eq. (5.41) is satisfied. Otherwise, the production increases or decreases exponentially.

5.6.3 Study of the Growth of Two Architectural Models

Here we study in particular the growing behavior of two widespread branched architectural models, with monopodial development (e.g., coffee tree representing the Roux model) and sympodial development (e.g., manioc representing the Leeuwenberg model).

5.6.3.1 Model with Monopodial Branching

This model has two categories of axes corresponding to the two PAs: main stem and branches. Each phytomer on the main stem has a leaf and a branch. Sinks are same for the two PAs.

A duration $t_a = t_x$ is set for the functioning and expansion times of the organs and a lifetime t_2 for axes of order 2 (branches). The plant demand and the biomass production stabilize for $t > t_2$ if the condition (Eq. 5.41) is verified. Indeed, since the lifetime of the leaves is t_a, the number of active leaves becomes constant and is: $N_a(i) = t_a \cdot (t_2 + 1)$ for all $i > t_2$. With the values of the parameters $t_a = t_x = 5$, $\varepsilon = 0.05$, $r = 30$, $p_a = 1$ and $p_e = 1$, the equality (Eq. 5.28) is checked. We have:

$A = 0.05 \times 2 \times 30$, we have: $\frac{1}{3} \times \left(\frac{5+1}{2} + 5 - 5\right) = 1$

With these parameters, production stabilizes and so does the Q/D ratio, which represents the trophic pressure. We show by simulation that the production depends increasingly on the lifetime t_2 of the branches. For $t > t_a$ and $t > t_2$, the larger the t_2,

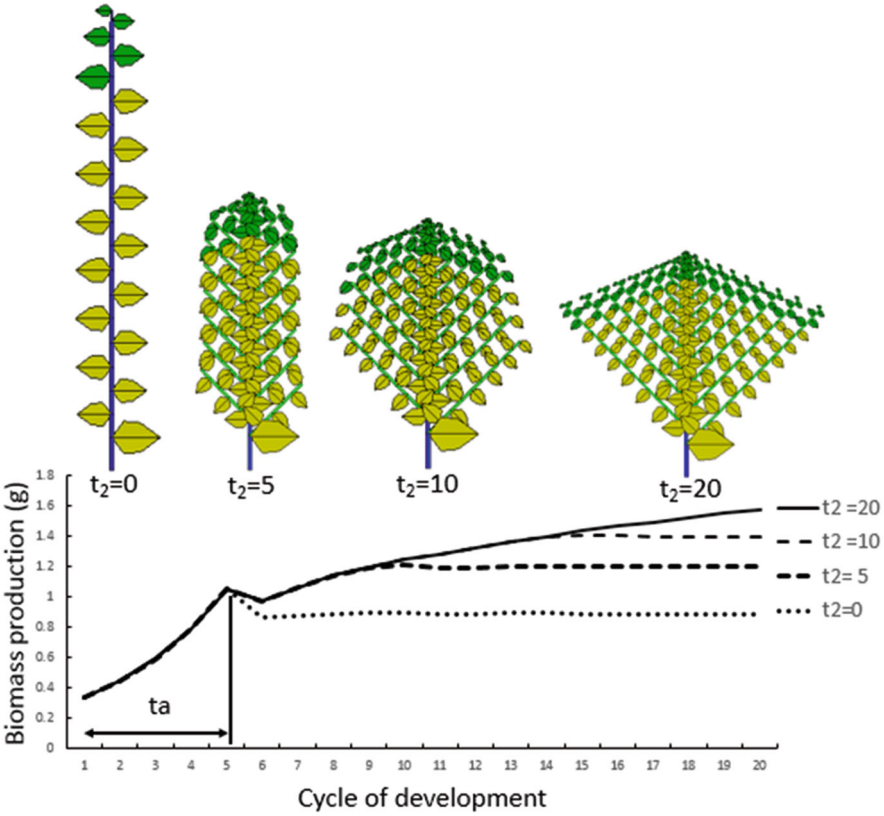

Fig. 5.26 Stabilization of the growth of the Roux model when the condition (Eq. 5.41) is verified. Yellow leaves are no longer functional. Beyond $t > t_a$, they are different lifetime values t_2 for the branches: $t_2 = [0, 5, 10, 15, 20]$. The value $t_2 = 0$ corresponds to the single-stemmed plant. As long as $t < t_a$, the plants have the same exponential growth. For $t > t_2$, the larger the t_2, the stronger the production at equilibrium, which is reached later, and the smaller organs are. Branched architectures correspond to the lifetime of the axes $t_2 = [0, 5, 10, 15]$ for the chronological age (CA) of 20 DCs with $t_a = 5$ and $t_x = 5$. Stabilization of the organic series is observed when the age of the plant exceeds the lifetime t_2 of the branches. Simulated plants are sorted in ascending order of weight (Color figure online)

the higher the production $Q(t)$. However, an equilibrium is reached when t is sufficiently large (Fig. 5.26). If t_2 is unlimited, the growth increases indefinitely.

Simulations in the model (Fig. 5.26) show that the volume of phytomers decreases when t_2 increases, while the biomass production increases. For $t_2 = 0$, the plant is single-stemmed, and the phytomers reach their maximum volumes. It should be noted that biomass production for all t_2 values is the same as long as $t \leq t_a$.

This fact is verified experimentally, for example in cotton (Fig. 5.27): pruned cotton is taller than branched cotton but weighs less. There is a change in the functioning when $t = t_2$. Below this ($t < t_2$), branched or pruned plants have the

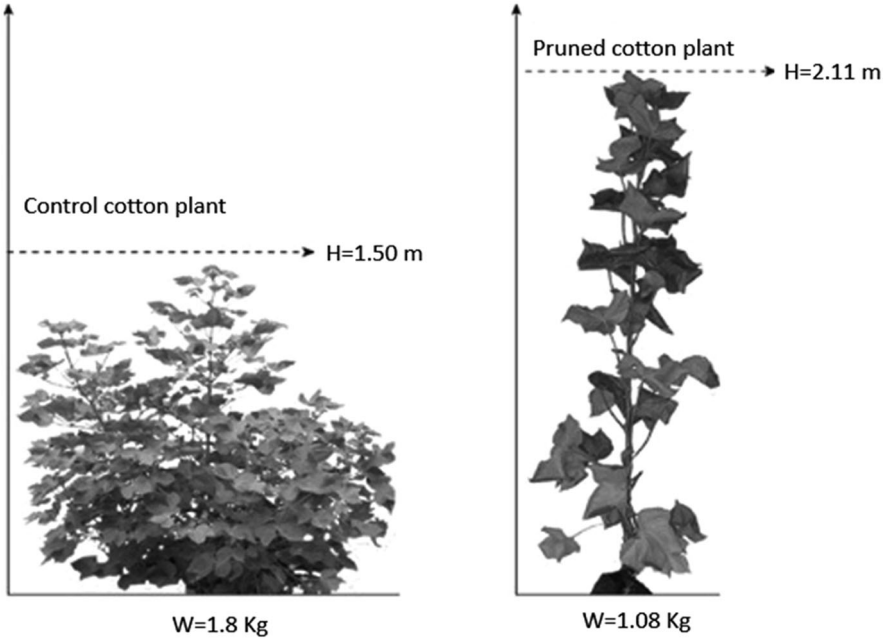

Fig. 5.27 Pruning experiments on cotton trees (personal communication, experiment by Li et al. 2010). The removal of axillary meristems from cotton stems results in an increase in the number and volume of phytomers on the main stem for the same development period. The weight of the control cotton plant (1.80 kg) is about twice as heavy as that of the pruned cotton plant (1.08 kg), whose height reaches 2.11 m, compared to 1.50 m for the control plant, with larger organs. According to GreenLab, if the duration of axis growth is longer than the duration of leaf functioning, the control plant weighs more than the pruned plant

same production (coffee tree, Fig. 5.26). Beyond that ($t > t_2$), plants with longer branches have larger biomass.

5.6.3.2 Model with Sympodial Branching

When condition (41) is verified, a limited demand is a sufficient but not necessary condition for stabilizing production. Thus, in the case of a sympodial model whose development is sympodial and exponential, it is possible to establish an equilibrium condition that can be verified by simulation. For $t_a = t_x$, if M (with $M > 1$) represents the number of branches per phytomer, this condition is written as:

$$\frac{E}{A} \cdot \left(\frac{M^{t_a}}{M^{t_a} - 1} \cdot t_a - \frac{1}{(M-1)} \right) = 1 \tag{5.44}$$

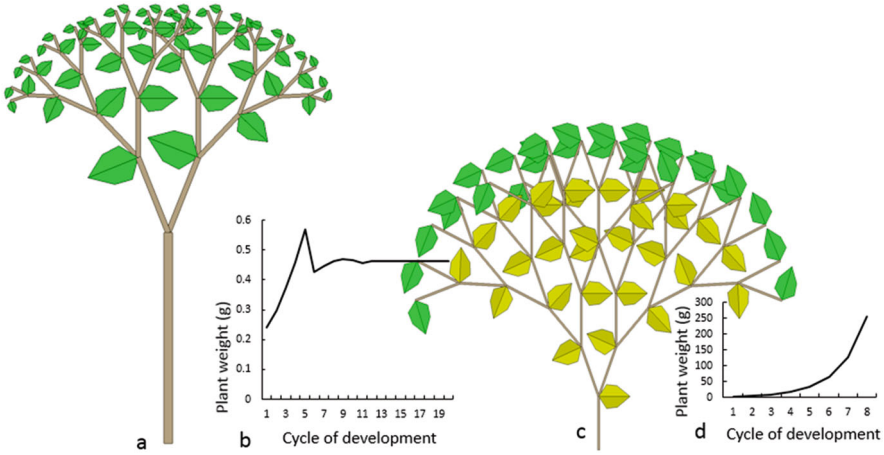

Fig. 5.28 Study of the behavior of a sympodial model in free growth. The duration of leaf function and organ expansion is 5 development cycles (DCs) here. The condition of Eq. (5.29) is checked for the values $M = 2$, $t_a = t_x = 5$, $r = 41.613$, $\varepsilon = 0.05$, and $P_p = 2$. Growth stabilizes, although the volume of phytomers tends towards zero. (**a**) Simulated plant at $t = 6$ DC. (**b**) Evolution of the produced biomass that stabilizes after 10 DC of the development. **c** here we set $t_a = t_x = 1$. The growth equation is written for the values $M = 2$, r = 5, $\varepsilon = 0.05$ and $P_p = 2$. $Q(t) = 2^{t-1} \cdot Q_0$, and the demand is $D(t) = 2^{t-1}$, so Q/D is constant, organs keep the same size, and growth is exponential

The equilibrium here depends on the number of branches per phytomer M (if $M = 1$, it can be simplified to a model with a single sympodial axis). Although the demand is growing exponentially, the foliar biomass produced per cycle is stabilizing, while organ volume is decreasing exponentially (Fig. 5.28a, b). In general, in this model, the development and growth are exponential. The organs can even be of constant biomass if Q and D have the same evolution, which naturally gives an exponential growth of the biomass (Fig. 5.28c, d).

5.6.3.3 Sink Source Organs and Stabilized Production Relationships

In the general case, a phytomer is a set of organs consisting of an internode, one or more leaves, and possibly several fruits. It is assumed here that all organs have constant sink values.

Equation (5.41) gives the condition of free growth at equilibrium. Each of the variables that constitute the coefficient A can be adjusted to achieve this equilibrium.

Figure 5.29a shows a case of equilibrium based on a complex phytomer consisting of one internode, two leaves, and six fruits. The architectural model here is a monopodial branched plant with a branch life span limited to $t_2 = 10$ DCs.

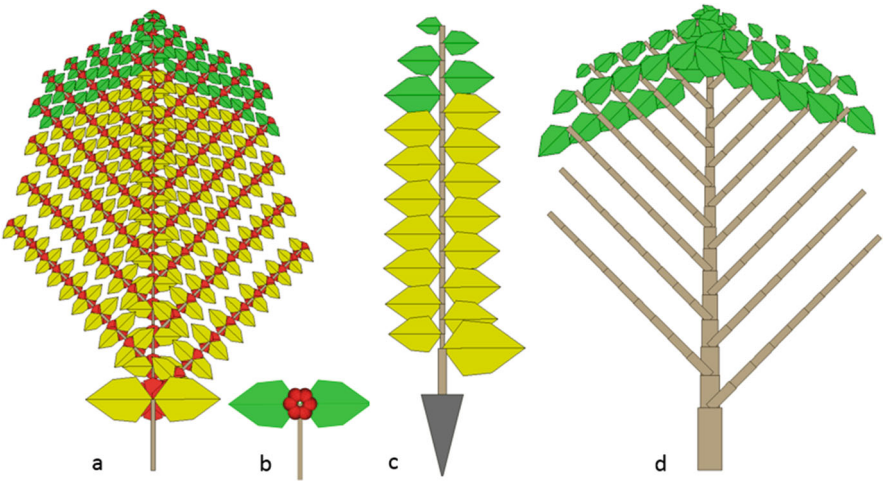

Fig. 5.29 Plants with complex phytomers, with secondary growth or root system. (**a**) Plant reaching a steady production with complex phytomers consisting of one internode, two leaves, and six fruits. (**b**) Detail of a phytomer. In this example, all the sinks of the organs are identical, only their numbers change. The expansion times are $t_x = 3$ DCs and the functioning lifespan of the leaves $t_f = 4$ DCs, and the branches $t_2 = 10$ DCs. Eq. (5.28) is checked for $r = 13.33$, with $\varepsilon = 0.05$. The demand for the expanding phytomer is $P_\varphi = 2 + 1 + 6 = 9$. $A = r \cdot \varepsilon \cdot P_\varphi$. Eq. (5.28) gives: $E \cdot \frac{na}{A} \cdot (\frac{t_x+1}{2} + t_a - t_x) = 1 \Rightarrow \frac{2}{13.33 \times 0.05 \times 9} \times (\frac{3+1}{2} + 4 - 3) = 1$. (**c**) We introduce a constant root sink $p_r = 4$. The sinks of the internodes and leaves are 1. The functioning and expansion times of the leaves are $t_a = 5$ and $t_{xa} = 5$. The expansion time of the internodes is set to $t_{xe} = 1$. The demand per cycle is therefore $D = 5 + 1 + 4 = 10$ and the growth is steady for the values of the chosen parameters. (**d**) The secondary growth on a branched model is visible. The parameters are $p_a = 1$ for the leaf sink, $p_e = 0.5$ for the internode sink, and $p_c = 0.5$ for the ring elements. We set: $t_a = t_x = 5$, $\varepsilon = 0.05$, $r = 30$, $t_2 = 10$, which gives a growth to the equilibrium

5.6.3.4 Special Sinks: Rings and Roots

In plants, there are particular sinks that do not correspond to well-located organs. They are the rings that ensure the secondary growth of the woody axes, and the roots whose architecture is complex and difficult to access.

Modeling of root system architecture has been a subject of research at CIRAD (Jourdan and Rey 1997), INRA (Pagès et al. 2004) in France, and CAU in China (Zhang and Li 2009). There are root architectural models (Atger and Edelin 1994) in their organizations. However, the notion of root phytomer does not exist in the literal sense. From an experimental point of view, the study of root systems is hampered by the difficulty of access. GreenLab considers the root system as a compartment with a variable sink, whose expansion can be indefinite. For some studied species (Chap. 9, beetroot, tomato, cucumber, etc.), the weight of the root system was available and was, therefore, integrated into the source–sink relationships. Figure 5.29c shows a single-stemmed plant whose growth is stabilized with source–sink parameters, including a root system treated as a constant sink.

Chapter 8 discusses the rings and provides the principles of secondary growth modeling in GreenLab. Here we consider the demand for the rings related to the architecture in the case where each functional leaf is associated with an element of ring. This element is also a sink. It has a shape of a cylindrical tube of biomass that travels along the edge of the axis from the leaf to the base of the tree. These sets of elements (pipes), grouped in bundles, extend from the ends of the tree axes to the base of the trunk, forming the rings. This model is known as the "pipe model" (Chap. 8). The demand for rings is the product of the number of active leaves multiplied by the sink strength of a ring element. Its sink strenght is constant and lasts for only one cycle. In this case, it is easy to define a production equilibrium as in the previous cases (Fig. 5.29d) to test the model's behavior.

5.6.4 Case of Rhythmic Growth

In the case of trees, the rhythmic development that forms GUs complicates the functioning. However, it is possible to study its behavior in two contrasting cases.

5.6.4.1 Synchronous Trees with Preformed Growth Units

The preformed part of the GUs is first formed during the year as a series of embryonic phytomers in apical meristems, in several DCs with negligible demand. A bud is thus formed. During its bud burst in spring, the sinks of the organs become effective, and there is a simultaneous expansion of all preformed phytomers (which are identical in our example here): a new GU is formed from the reserves of the previous year. The leaves and pith of the internodes no longer evolve, and the shape of the GU is stabilized. Its photosynthetic functioning produces the biomass in reserve for the following year. The expansion period is considered negligible compared to the functioning period. Without loss of accuracy, all functioning cycles can be concentrated in a single cycle that aggregates the expansion of the GU and cumulative photosynthesis. Its development scheme is:

- a development period of several DCs to form embryonic phytomers of the GU;
- a DC to ensure the expansion of the GU and its subsequent production;
- a DC to mark the winter pause (by convention).

Trees such as chestnut trees or maple trees fit well into this framework. Finally, this type of functioning is like that of the continuously growing shrub, but on a double scale. All the phytomers of the GU behave as if there were only one meta phytomer composed of an internode and a leaf, and the growing conditions are those of a shrub with $t_a = 1$ and $t_x = 1$ (Fig. 5.30a).

The simplified growth equation is written as Eq. (5.39):

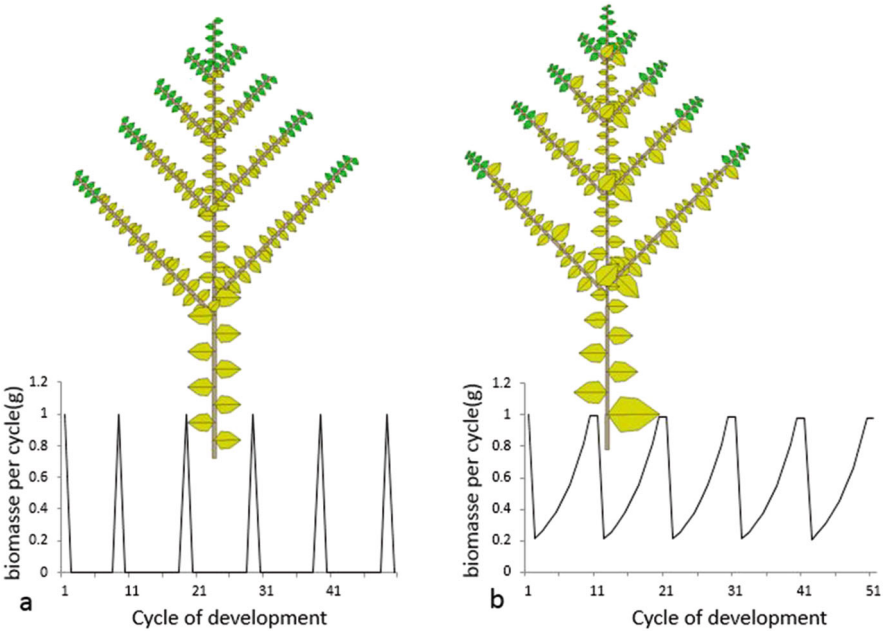

Fig. 5.30 Two theoretical cases of possible stabilization in the rhythmic growth of trees with an annual growth divided into 10 development cycles (DCs). In both cases, a cyclic stabilization of production can be achieved for a set of parameters. The stabilized cycles of production $Q(t)$ are displayed below the corresponding trees. (**a**) Growth from a preformed GU. Development and growth are not synchronized (Chap. 6). Growth is delayed. Embryonic phytomers preformed in 9 DCs have simultaneous expansion at DC 9, and therefore have the same volume. DC 9 concentrates the photosynthesis into one cycle. A pause (DC 10) separates two years (Parameter $r = 10$). (**b**) The phytomers have been formed one by one. Development and growth are simultaneous. Phytomers have different volumes depending on the trophic pressure Q/D at the time of their creation. At the end of the GU, all the leaves stop working together, and a pause ends the year (Parameter $r = 46.9$)

$$Q(t) = \left(\frac{E}{A}\right)^{t-1} \cdot Q_0$$

It gives the growing behavior of the model and the equilibrium condition $E/A = 1$.

5.6.4.2 Synchronous Trees with Neoformed GUs

The phytomers produced by meristems immediately expand after their formation. It is assumed that the leaves remain functional until $t = t_a$ whatever their time of appearance. The functioning of the first leaf of the GU of rank 1 lasts t_a DCs, the second of rank 2 lasts $t_a - 1$ DCs, and the functioning of the last leaf of rank t_a lasts only 1 DC. In addition, the expansion time of the phytomers $t_x = 1$ is fixed. Under these conditions, the growth is driven by Eq. (5.40) established previously.

To reach stabilized cyclical growth, A must be the solution of Eq. (5.40):

$$Q(t) = \frac{E}{A} \cdot \left(1 + \frac{E}{A}\right)^{t-1} \cdot Q_0$$

Which gives the following equation to solve (setting $Q_0 = 1$):

$$A + E - \left(\frac{A^{t_a}}{E}\right)^{\frac{1}{t_a - 1}} = 0 \tag{5.45}$$

We have $A = r \cdot \varepsilon \cdot P_p$; we can choose r as unknown and set: $E = 1$, $\varepsilon = 0.05$, $P_p = 2$, $t_a = t_x = 9$ as an example.

The value $r \approx 47$ gives a stabilized cyclical growth rate each year (Fig. 5.30b).

These behavioral studies are useful for understanding plant growth and monitoring the proper functioning of simulation software.

5.7 Behavior of the Model: Case of Limited Growth

The production area *Sp* limits the growth. When plants are grown at a high planting density d on a surface S_c, the ground is completely covered by the foliage, and the available ground area per plant tends towards the value $Sd = S_c/d$, which also becomes the production area Sp. In this case, biomass production per plant is no longer proportional to its leaf area *Sf*, as in the case of free growth, but to the available ground area per plant *Sd*. The leaves are in fact in excess compared to the produced photosynthesis.

According to Eq. (5.18), there is necessarily an upper limit value for biomass production per plant in each cycle:

$$Q(t) < \frac{E \cdot Sp}{r} \tag{5.46}$$

There are, therefore, two possibilities (Fig. 5.31) for the plant to reach an equilibrium during the growth. One is in free growth, and the other is in limited growth. The first equilibrium is metastable and gives dwarf plants; the second is limited by an upper limit which corresponds to normal growth conditions, constrained by the available area *Sp* per plant in the stand. This upper limit does not depend on the plant architectural model, but the true limit Q_l depends on it and is found by iteration on Eq. (5.18). This limit is related to the solution of Lambert equation.

The evolution of the Q/D ratio (trophic pressure) controls the size of the phytomers. Figure 5.32 shows the architecture of three plants single-stemmed, monopodial with $t_2 = 10$ and sympodial, respectively. The influence of *Sp* on the

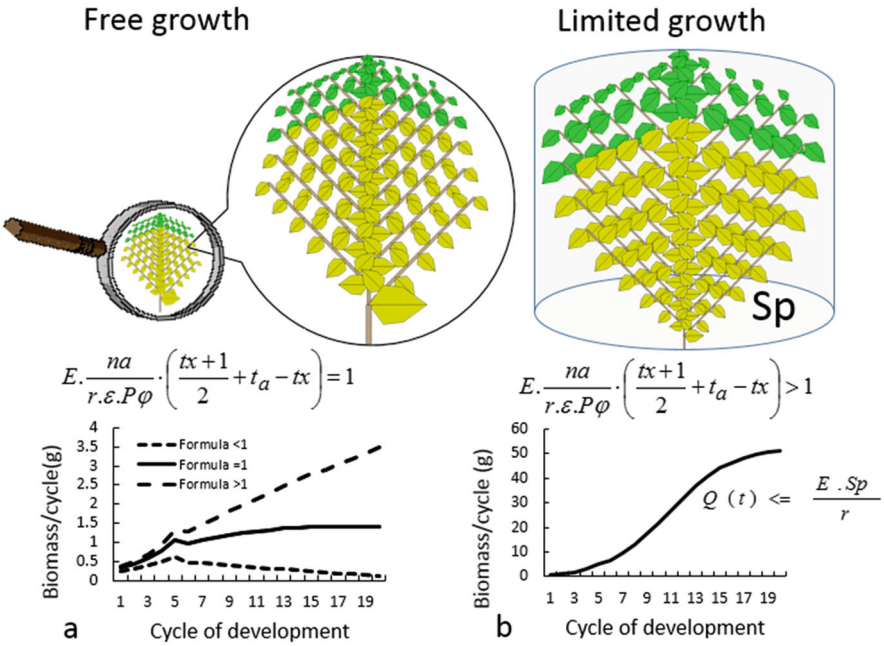

Fig. 5.31 Two cases of stabilized growth and development. The branches are limited to a development of 10 phytomers. The functioning of the leaves is limited to five cycles. Plants (**a**) and (**b**) are on the same scale. Note that the first case gives dwarf plants in metastable growth equilibrium. (**a**) *Sp* is very large and the relationship (Eq. 5.27) $\frac{(t_a+1)}{2}\cdot\frac{E}{A}=1$ is verified: it is the free growth proportional to the leaf area. It should be noted that the volume of the organs decreases from the seed to stabilize with the organic series. If the equation value is smaller or larger than 1, the growth decreases or increases exponentially. (**b**) *Sp* is small and $\frac{(t_a+1)}{2}\cdot\frac{E}{A}>1$. This is the growth limited by the light intercepted with $Q(t)\leq\frac{E}{r}\cdot Sp$. It should be noted that the volume of organs grows from the seed to stabilize

growth limitation means that the biomass produced per cycle reaches an equilibrium, whatever the architectural model. But the demand also stabilizes, leading to the organic series stabilizing from the top. For the single-stemmed plant (Fig. 5.32a), it stabilizes when $t > t_a$. The crown of the stem becomes invariant. For the monopodial plant (Fig. 5.32b), whose branches stop their development after t_2 cycles, the demand stabilizes after $t_2 + t_a$ cycles. The crown of the plant also becomes invariant. For the sympodial plant (Fig. 5.32a), whose development is exponential (2^t), the architecture becomes fractal, because the biomass produced per cycle is stabilized.

The architecture of the plant certainly influences its production. In the model, this is traduced by the fact that *Sp* depends on the bearing of the tree (columnar, tabular).

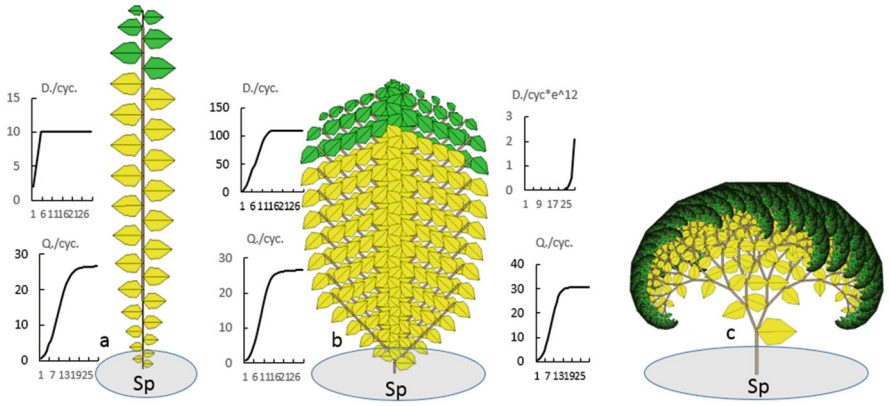

Fig. 5.32 Architectures of three plants. (**a**) Single-stemmed, (**b**) Monopodial with $t_2 = 10$, and (**c**) Sympodial dichotomous with $t_a = t_x = 5$ DCs, $p_a = p_e = 1$, $E = 1$ and $r = 15$. The plants (**a**) and (**b**) have a production per cycle that stabilizes because of $Sp = 500\ cm^2$. It is bounded by ($E{\cdot}Sp/r = 33$). The plants (**a**) and (**b**) have a stabilizing demand. The crowns of these two plants become invariant. Plant (**c**) has an exponentially growing demand. The architecture becomes fractal

5.8 Influence of Environmental Parameters

5.8.1 Influence of the Factor E

In ecophysiology, the factor E links the growth to the resource related to the environmental parameters. It is associated with the parameter r, which characterizes the efficiency of converting this resource into biomass. The biomass $Q(t)$ synthesized at cycle t is proportional to parameter E (Eq. 5.18). Relationship Eq. (5.41) shows that growth can only occur if E exceeds a certain threshold that depends on source-sink parameters.

In real conditions, the parameter E can change with each growth cycle and is then defined as a variable $E(i)$. In the absence of data about the environmental variables and in the absence of strong stress, the factor E can then be normalized to 1; the parameter r is used for calibration, and the study of source–sink relationships remains unchanged. This is of great interest, as the growth and architecture become independent of environmental parameters. It becomes possible to study the source–sink relationships of a plant collected in an environment (light and temperature) whose history is unknown.

5.8.2 Influence of the Parameter Sp

The parameter Sp makes it possible to solve the growth at each time step, by balancing the two members of Eq. (5.13) if the weight of the plant and its leaf area is known or estimated.

$$Q(t) = \frac{E \cdot Sp(t)}{r} \cdot \left(1 - \exp\left(-k \cdot \frac{Sf(t)}{Sp(t)}\right)\right)$$

In practice, it is not possible to calculate the value of $Sp(t)$ at each time step. To solve this problem, an empirical function is chosen that follows the evolution of $Sp(t)$ as a function of CA, with a small number of parameters that can be identified by an inverse method. Two cases are considered.

5.8.2.1 Cases of High Planting Densities

This is generally the case for field crops; the number of plants per m^2 depending on the type of plant varies from a few units to a few dozen.

At germination, the ratio $Sf(t)/Sp(t)$ is small and Eq. (5.12) becomes:

$$Q(t) = \frac{E \cdot k \cdot Sf(t)}{r}$$

The value of Sp does not play roles. When this ratio increases, it suddenly tends towards the limit of the available surface area per single plant $Sd = S_c/d$ given by the cultivated area Sc of the stand and the planting density d and we find:

$$Sp \approx Sd.$$

The solution of Eq. (5.13) is, therefore, $Sp(t) = Sd$.

When d increases, the area Sd decreases as $Sd = S_c/d$. Assuming unchanged source–sink relationships, the biomass q produced by the individual plant decreases and the biomass Q produced by the stand increases. This value tends towards a maximum $Q_l = E{\cdot}Sd/r$.

Figure 5.33 shows a simulation of the relationship between the biomass of the individual plant and those of the stand according to the planting density.

This behavior has been well verified for field crops. A verification of the relationship between the biomass produced by a single plant and that produced by its stand for a planting density is given with beetroot (Fig. 5.34, Lemaire et al. 2008).

The weight of a single plant depends on the planting density, but the harvest of the stand per m^2 is the same.

Repeated experiments over several years and on various crops—tomato (Dong et al. 2007, 2008), maize (Ma et al. 2008), beetroot (Lemaire et al. 2008), and wheat (Kang et al. 2008)—confirm the suitability of the model for agronomy. The leaf area and weight of the plant are available on several different dates. We can, therefore, find the numerical values of the parameters r and Sp by an inverse method which best fits Eq. (5.12).

For example, Fig. 5.34 shows that the biomass production of a beet (Lemaire et al. 2008) grown at a density $d = 5$ plants/m^2 (giving $Sd = 2000$ cm^2) is adjusted for the

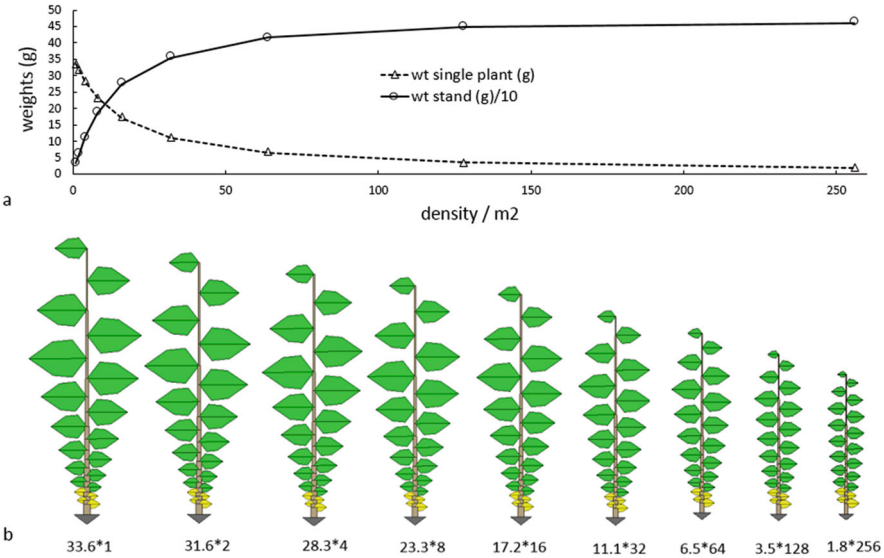

Fig. 5.33 The parameters of the simulated plant at 20 development cycle (DC) are: $t_a = 15$ DCs, $t_{xa} = t_{xi} = 5$ DCs, $t_{xt} > 20$ DCs. $p_a = 1$, $p_e = 0.5$; p_c (ring) =0.5; p_t (root tape) = 4. Starting from a planting area S_c =10,000 cm^2 (1 m^2), the planting density is doubled each time from $d = 1$ to $d = 256$. The volume of the individual plant gradually decreases. (**a**) The biomass produced per individual plant (triangle marker) and the biomass produced/10 plants by the stand (round marker) are displayed. This tends towards a maximum: $Q_1 = E{\cdot}S_c/r = 500$ g. (**b**) The architecture of the plant is displayed according to the planting density

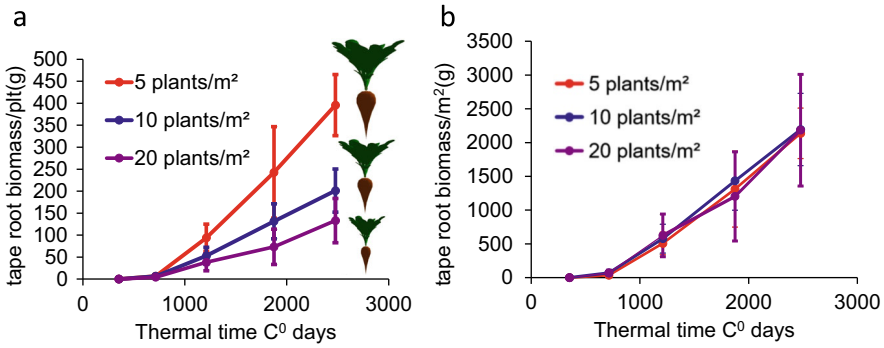

Fig. 5.34 (**a**) Weight of the taperoot of an isolated plant for three densities (5 plants/m^2, 10 plants/m^2, 20 plants/m^2) and for three growth dates. (**b**) weight of the harvest per m^2 in tape roots for the three densities (5 plants/m^2, 10 plants/m^2, 20 plants/m^2) and for the three growth dates

values: $r = 177$ and $Sp = 2055$ cm^2, by the inverse method. The Sp and Sd values are, therefore, very close. The model can retrieve the planting density only from the leaf area and the biomass produced. Figure 5.35 clearly shows the behavior of the two-stage growth as shown in Fig. 5.16. In the first stage (DC $<$ 40), which is

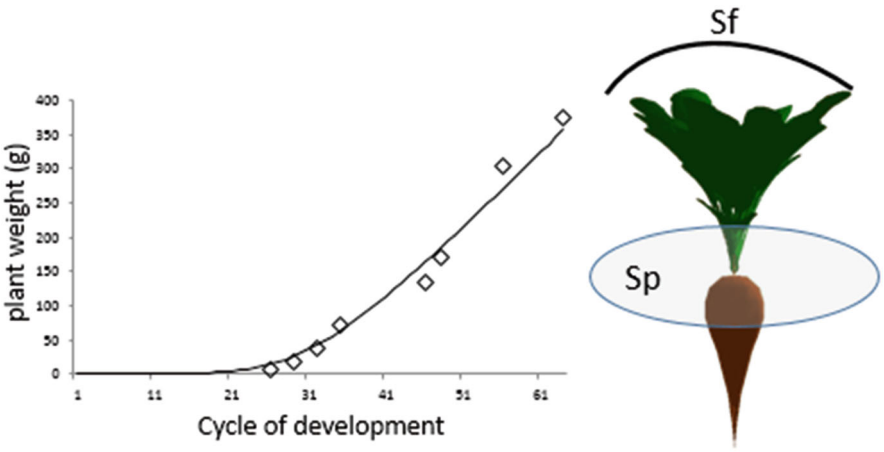

Fig. 5.35 Adjustment of the beet weight according to the leaf area during the growth, grown at a density of 5 plants/m^2 by Eq. (5.12). The solid line and the symbols (◊) represent the calculated data and the observed data, respectively. The average available surface area per plant is, therefore, $Sd = 2000$ cm^2. There are eight sampling dates (in DC). The leaf area is measured as well as the weight of the plant with the tape-root (average of 18 plants per date). The assessed parameters r and Sp of the growth equation are $r = 177$ and $Sp = 2055$ cm^2. The value of Sp corresponds well to the value of Sd (5 plants/m^2). (Source: Data from Sébastien Lemaire, ITB, 2010)

exponential growth, it is the leaf area Sf that drives the process; in the second stage, which is linear growth, it is the available area Sd that limits the production with $Sp = Sd$.

The numerical value of Sp is a hidden parameter in the production Eq. (5.17) of GreenLab.

It is easier to consider the weight of a plant (easily measurable) for computations rather than the production of biomass per cycle. The latter has a sigmoidal shape (Fig. 5.32) and its integration gives precisely the weight of the plant.

In Chap. 9, experiments confirming the above results are shown on tomatoes, maize, beet, and wheat.

They are an experimental validation of GreenLab. In the case of high planting density, Sp is always close to Sd (Fig. 5.36). When the plants are isolated, the value of Sp becomes lower than the value of Sd. It corresponds to the value of the projection of the leaf crown on the ground. At the young stage, the assessed value of Sp is very high (all leaves see light) and is not actually computable by the inverse method.

5.8.2.2 Case of Low Densities: Variation of *Sp*

In cases of low densities, the problem is complex. Between the initial free growth and the limited growth, there should be a progressive evolution of Sp which starts from a high initial value, decreases to a minimum under the effect of the self-shading

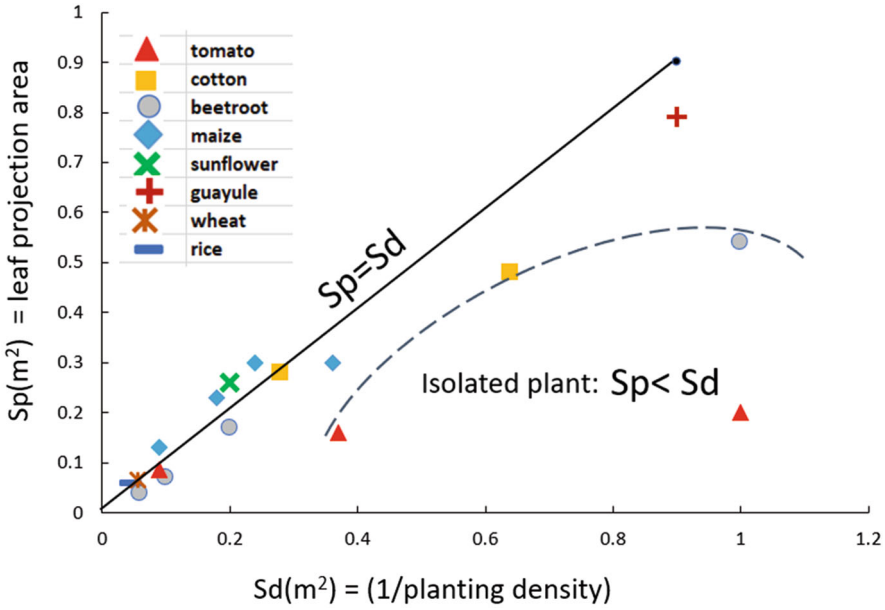

Fig. 5.36 Comparison between the available areas *Sd* by the planting density *d* ($Sd = 1$ m^2/plant) and the calculated production areas *Sp* for four types of plants: tomato (○), maize (Δ), beet (◊), wheat (*). All dots are around the bisector for high planting densities ($Sp = Sd < 0.3$ m^2/plant which corresponds to a planting density > 5 plants/m^2), or for crowns in contact. Isolated plants move away from the bisector ($Sd > Sp$). *Sp* no longer corresponds to an available surface, but to a surface that balances production with the leaf surface considering self-shading. (Sources: data from Sébastien Lemaire (2010) in ITB, Ma Yun-Tao (Ma et al. 2008) and Dong Qiao-Xue (Dong et al. 2007, 2008) in China Agricultural University (CAU) and Feng Lu (Feng et al. 2013) in CIRAD)

of the leaves, then increases under the effect of the extension of the crown projection. If the thickness of the latter is sufficient to obscure the light, then the surface of projection on the ground *Sh* of the crown is an estimate of *Sp*. If the plant is isolated and the growth is indefinite, *Sp* grows indefinitely. If it meets its neighbors, then the production surface stabilizes due to the stabilization of the projection surface on the ground of the crown.

Olivier Taugourdeau (Taugourdeau et al. 2013) (CEF, Canada) was able to estimate the value of the projection surfaces on the ground *Sh* of sugar maple tree canopy during its growth. They are approximated as ellipses whose two axes are measured over a period of 10–80 years (see Chap. 10). The adjustment of the organic series can be achieved only by assuming that the evolution of *Sp* follows a bi-parametric U-shaped curve, the parameters of which are to be assessed at the same time as the other source-sink parameters of the maple. The comparison of the optimized *Sp* values with the estimated ground projection surfaces *Sh* is satisfactory, and experimentally validates GreenLab for trees over a long growth time. After 20 years, the LAI is strong and, as expected, the measured crown projection surfaces

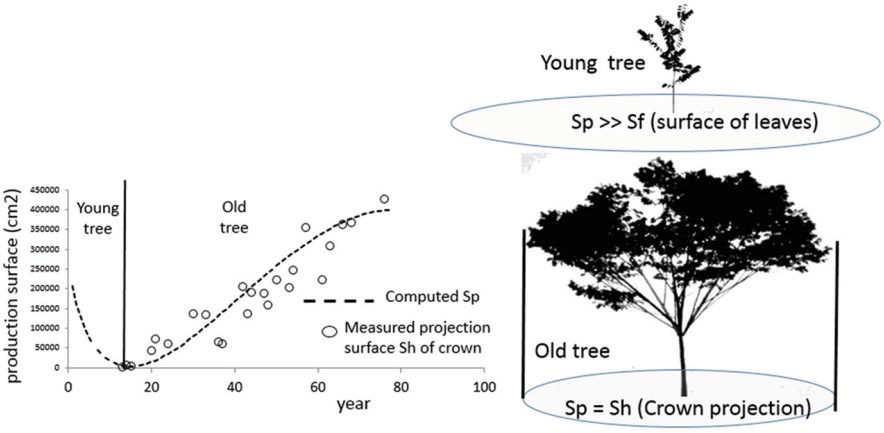

Fig. 5.37 Evolution of *Sp* along the chronological age (CA). Comparisons between *Sh* values estimated from measurements of maple crown projection surfaces (circles) and *Sp* values calculated by the inverse method (dashes) by adjusting the organic series of GU. There is a satisfactory agreement between the prediction and the observations. For young stages, *Sp* is not measurable, but its value is calculable. (Source: Data from O. Taugourdeau (2013), CEF, Canada)

are acceptable *Sp* solutions (Fig. 5.37). But at the young stage, no estimation of *Sp* by direct measurement is possible. Only the inverse method can optimize its value.

The study of Teak growth (Chap. 10) has shown the behavior for the evolution of the parameter *Sp* which follows a U-shaped curve as a function of time. The formulation of this U-curve is explained in this Chap. 10.

5.8.2.3 Pool of Reserve Implementation

In the current version of the Gloups software, the GreenLab model has a simple common pool with no storage. At each growth cycle, a quantity of biomass is produced by the photosynthetic organs (leaves, sheaths, etc.) and is placed into a common pool which is redistributed in its entirety to the expanding organs. There are, therefore, no remobilizable reserves over several cycles except in the following two cases:

- At the beginning of growth, the seed gives up the quantity Q_0 to create the young seedling. This can be given up to the plant either in one cycle or over several cycles (see Sect. 5.6.1.1, Fig. 5.20d). In this case, the quantity given up in each cycle is supposed to be formulated as: $\Delta q_0(i) = Q_0 \cdot (1 - k_o)^{i-1} \cdot k_o$ which decreases exponentially until all the seed's reserve is exhausted. k_o is a damping coefficient. If it is zero (usual case), all the biomass is given up at the time of the first growth cycle.

- The phenomenon of remobilization (see Chap. 9, Sect. 6.10 on rice) allows the organs to return part of their biomass to the common pool when their individual operating time is exceeded.

The rule is that all biomass in the common pool is taken up by the expanding organs during the growth cycle. If photosynthesis is suppressed, growth stops. In the case of continuous growth, a single cycle without photosynthesis is enough to cause the death of the plant. In the case of rhythmic growth (trees) in the autumn, the biomass of the common pool is put on hold, through structural pauses for the renewal of growth in the following spring (see Sect. 6.4.1).

It is possible to implement a more flexible system that incorporates a reserve pool, denoted as Q_s, which accumulates biomass at each growth cycle in proportional to the photosynthetic production. In the case of photosynthesis stops, the system can continue to support growth by drawing from the reserve pool.

Unfortunately, it seems very difficult to validate such a system by agronomic experiments. Anatomically, the reserves are stored as starch grains within cell vacuoles, taking the place of water. The volume and density of the cells change little and we cannot directly measure the reserves by deforming the volumes of the organs in the organic series. Since the profiles of the organic series being unaffected, we cannot estimate the functioning of the reserves by an inverse method. Indeed, given that the fits of the series are of good quality with a common pool system without reserves, there is not enough information left to refine the model with a reserve compartment.

Let Q_s be the common pool, we can conjecture the need to define two parameters a and b that are used, respectively, for filling and emptying the common pool Q_s. We pose:

$$\Delta Q_s(i) = a_{Qr} \cdot Q(i-1)/D(i)$$

$Q(i)$ is the biomass synthesized at DC i and $\Delta Q_s(i)$ is the amount added to the reserve pool Qs. a_{Qr} is the sink of the reserve compartment. The amount $Q(i) - \Delta Q_s(i)$ is used for organ expansion in cycle i. If photosynthesis is removed, the reserve pool returns the quantity $b_{Qr} \cdot Q_s(i)$ to the common pool at each cycle. b_{Qr} is the emptying coefficient of the reserve pool. There remains the quantity $(1 - b_{Qr}) \cdot Q_s(i)$ in the reserve pool.

Such a system with parameters a_{Qr} and b_{Qr} cannot be estimated using the organic series by an inverse method. But the values can be fixed a priori for simulation purposes. Probably experiments with cuttings or pruning would be good candidates to study the effect of reserve behavior. For example, during pruning, the biomass comes mainly from the reserves stored in the root system.

For the purpose of this study, a subroutine in Gloups was developed to simulate the behavior of the plant interacting with a reserve compartment (Fig. 5.38). The light radiation $E(i)$ at cycle i varies throughout the growth period, with values ranging from 1 to 2. A threshold $Eo = 1$ is set below which photosynthesis stops and therefore the reserve pool feeds the common pool.

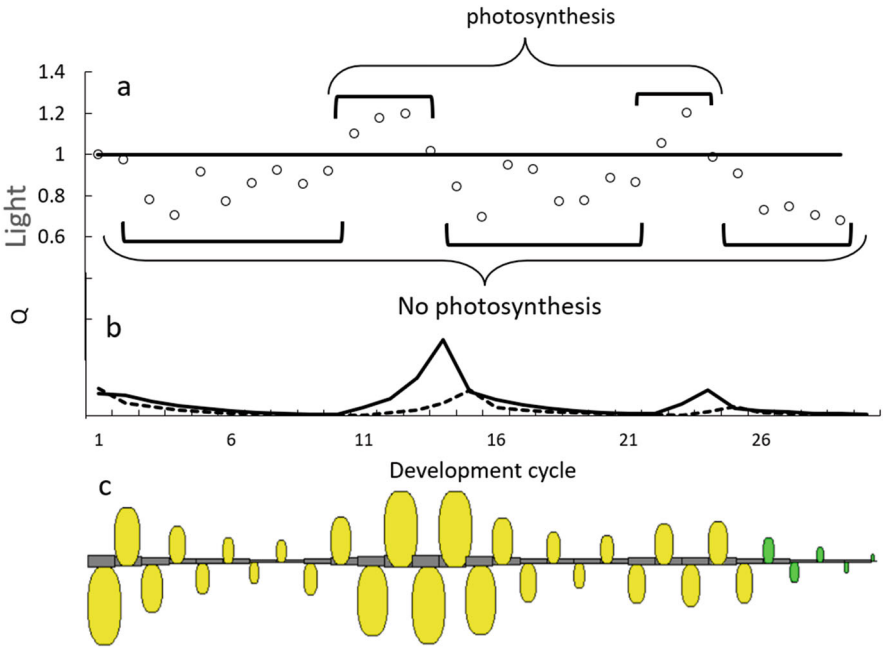

Fig. 5.38 Effect of the reserve pool: (**a**) Occurrence of photosynthesis during growth. (**b**) Parallelized evolution of the biomasses of the common pool and the reserve pool. (**c**) Plant growth resulting from the action of the reserve pool (biomass production solid line, reserve pool dotted line)

The parameters of the system are $t_a = t_x = 5$; $Q_0 = 1$; $r = 5$; $Sp = 2000$; $p_a = p_e = 1$ (sinks of the leaf organs and internodes); $a_{Qr} = 5$ (sink of the reserve compartment); $b_{Qr} = 0.5$ (emptying coefficient of the reserve compartment).

Between DC 1 and DC 10, there is no photosynthesis; the growth is ensured by the seed, which feeds the reserve pool that is being empty. Between DC 11 and DC 15, DC 22 and DC 24 photosynthesis is active and the reserve pool fills up. Between the DC 16 and DC 21, DC 27, and DC 30, the reserve pool is getting empty. Without the reserve pool, growth would have stopped after the first cycle.

5.9 Application of Organic Series Analysis on Cultivated Plants

The adequacy of the GreenLab model to the crops is shown below by the quality of the fittings obtained when compared to the observed organic series within the model. These adjustments are more significant on the performance of the GreenLab model than 3D plant simulations that only provide a geometric appearance. Fitting the

organic series with the GreenLab model using the inverse method is explained in Chap. 9.

5.9.1 Plasticity of Organic Series

Among the collection of plant species studied, a high variability was observed in the profile of organic series, i.e., the distribution of organ volumes by rank along the stem. This is fully explained by the source–sink interactions during the growth. The evolution of supply and demand (trophic pressure) literally sculpts plant architecture. It is omnipresent in the form of organic series.

The volume of an organ (see Sect. 4.2) depends on:

- The expansion time t_x;
- The sink function $P_o(x) = p_o \cdot F_o(x)$, where p_o is the sink strength of the organ and $F_o(x)$ is the variation of the sink strength normalized to its mode. This function is empirical. Its formulation is chosen to best capture numerical variations in observed sink strength.
- The evolution of the supply-to-demand Q/D during the expansion of the organ.

In the plants studied, the duration of organ expansion varies significantly. Often constant (cotton, tomato), it may depend on its position from the base in the organic series (sunflower, beetroot). Another example is that of leaves, which is almost immediate (2–3 DCs) for grasses such as wheat or rice, and about a hundred DCs for sunflower.

For internodes, the primary growth (the pith) is quite short (a few DCs). In herbaceous plants, it can be delayed. In this case, a rosette is formed before the elongation of the internodes of the stem. In woody plants, secondary growth is effective if the axis is not dead, it can occur on the trunk for hundreds of years.

The flowers can be in a lateral or terminal position on the axes. Fruits often have delayed expansions (cucumber).

In GreenLab, only the weight of the roots is considered if they exist. They are modeled as a compartment with a sink function that is active throughout the growth. If the weight of the roots is not measured, it is considered not to disrupt the internal source–sink relationships inside the shoots, which allows the aerial part to be studied independently (see Chap. 9).

Sink functions are expressed during the expansion time of the organs. They are hidden in the architecture and can only be estimated by the inverse method by fitting the organic series. Most often, their shape is an asymmetrical bell curve sink adjusted by a beta law. Exceptionally, in plants such as peppers or tomatoes, fruit expansion can be monitored and measured directly using diameter–weight allometries. The observed sink variations, when compared to those calculated by the inverse method, are found to be close, which validates the sink model. This approach avoids laborious growth monitoring.

5.9.2 *Organic Series and History of Plant Growth*

Organic series taken from the architecture of a plant implicitly contain the history of the evolution of its functioning. Their analysis allows to calculate the source-sink parameters and thus to reconstitute the supply and demand evolution of the plant during its growth.

Figure 5.38 shows the fittings by the GreenLab model of the organic series of leaves on the stems of five cultivated single-stemmed plants, whose profiles are different and characteristic of their specific functioning.

The first three plants in Fig. 5.39 have indefinite growth and the last two have finite growth, which ends with terminal flowering. All these plants begin with exponential growth, which is well simulated by the model. Projection areas are limited by planting density, which limits biomass supply. The senescence of the organs eventually limits the demand. Growth then quickly becomes stationary, resulting in the following results:

- Monopodial cotton (Li et al. 2010) ends up replicating the same phytomer. Leaves have a constant functioning duration. The profile of the top of the organic series of leaves becomes invariant. The newly expanding leaves at the beginning are small (Fig. 5.38a);

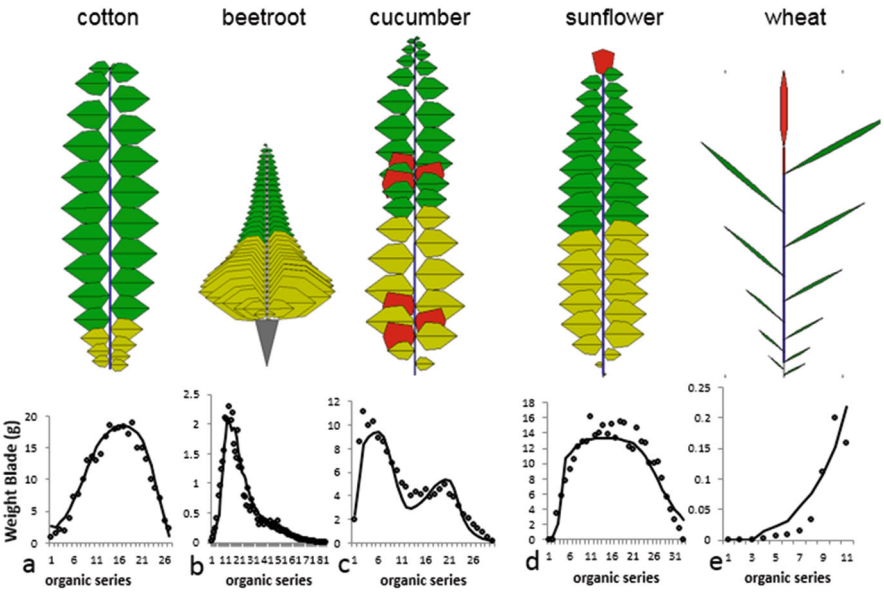

Fig. 5.39 Observations (dots) and fittings (lines) by the GreenLab model, organic series of leaves on the stem in five cultivated plants. There is a high degree of plasticity in the profiles of the leaf organic series according to the species. They depend on source–sink interactions between organs. (**a**) Cotton stem. (**b**) Beet rosette. (**c**) Cucumber stem. (**d**) Sunflower stem. (**e**) Wheat stem

- The root sink of the beetroot (Lemaire et al. 2008), initially negligible, is becoming increasingly important and concentrates all the demand. It eventually prevents the expansion of new created leaves that remain embryonic (Fig. 5.38b);
- Cucumber fruits (Mathieu et al. 2007, 2012) are an important sink. They lead to the abortion of the new fruits during their activity, until the end of their expansion. Fruiting can then resume. The demand for the fruits inhibits the growth of new phytomers and shrink the leaves. The position of the fruits depends on supply/demand ratio (Fig. 5.38c);
- The expansion of sunflower organs (Rey 2003) is done over a very long period (90 DCs). Leaves have variable functioning duration from the base of the stem. The appearance of the capitulum creates a new, strong sink. This slows down the growth of the last leaves, which remain small. If the capitulum is cut off at birth, these last leaves become larger (Fig. 5.38d);
- In wheat (Feng et al. 2013), the leaf expansion time is very short (2 DCs). The last leaves are therefore the largest, because the sink of the terminal ear has no influence, since they have already completed their growth (Fig. 5.38e).

These five examples will be presented in detail in Chap. 9.

5.10 Conclusion

The architecture of a plant depends not only on the activity of the meristems that generate its development but also on the biomass produced by the leaves and its distribution in the structure. The volumes and sizes of organs are dependent on the simultaneous evolutions of the demand D and the biomass production per cycle Q, and more specifically, on the trophic pressure (Q/D ratio).

The botanical automaton produces the cohorts of organs (organs of the same physiological and chronological age) which, together with their sinks, allow the computation of the plant demand. The architecture of any plant that meets the criteria of PA and the common pool can be decomposed into organic series, which contain the history of growth.

The study of the mathematical model makes it possible to identify two modes of growth: free growth (no competition with neighboring plants) and limited growth.

In free growth, biomass production is proportional to the leaf area. This situation is realized in the early stages of growth and results in exponential growth. All the leaves of the young seedling intercept the light.

In the case of high planting densities, the available area per plant is limited and a double limitation in the search for the light by the leaves occurs. The leaves of one plant overlap with each other and meet those of neighboring plants. The limited growth occurs and depends on the light intercepted by the foliage, which corresponds to its shadow on the ground, the sun at its zenith. This can be calculated using the notion of production area Sp, which is experimentally validated. In the case of high planting density d on a cultivated area S_c, the growth gradually becomes linear

and proportional to the surface area available per plant *Sd* ($Sd = S_c/d$). GreenLab computes a production area $Sp \approx Sd$ by an inverse method, which is a validation of the model (see Chap. 9).

The *Sp* production area method also ensures the passage from the individual plant to the stand level, and thus bridging the junction between a functional–structural model and a physiological crop model (Chap. 11). In addition, *Sp* is the solution of the production equation, which avoids calculating the interception of light by computer methods that use ray-tracing or radiosity on 3D models of simulated plants, a process that is difficult to implement in practice despite its academic interest.

The deterministic model of a functional plant, the subject of this chapter, is only found on single-stemmed plants such as maize and sunflower. But the more general stochastic model has a similar behavior (Chap. 6).

Validation of the model on several crops and inverse methods for computing the source-sink parameters of GreenLab from measurements on organic series are presented in Chaps. 9, 10 and 11).

References

Atger C, Edelin C (1994) Premières données sur l'architecture comparée des systèmes racinaires et caulinaires. Can J Bot 72(7):963–975

Buis R, Barthou H (1984) Relations dimensionnelles dans une série organique en croissance chez une plante supérieure. Rev Biomath 85:1–19

Li D, Letort V, de Reffye P, Zhan Z-G (2010) Modeling branching effects on source-sink relationships of the cotton plant. In: Li B.-G., Jaeger M., Guo Y (ed) The third international symposium on plant growth modeling, simulation, visualization and applications (PMA 09), 9-13 november 2009, Beijing, China. Los Alamitos, IEEE Computer Society, pp 293–302

Dong Q-X, Louarn G, Wang Y-M, Barczi J-F, de Reffye P (2008) Does the structure function model GreenLab deal with crop phenotypic plasticity induced by plant spacing? A case study on tomato. Ann Bot 101(8):1195–1206

Dong Q-X, Wang Y-M, Yang L, Barczi J-F, de Reffye P (2007) GreenLab-tomato: a 3D architectural model for tomato development. N Z J Agric Res 50:1229–1233

Feng L, Rey H, Mailhol J-C, Kang M-Z, de Reffye P (2013) Concept and calibration of virtual wheat including stochastic tillering. In: Risto Sievänen, Eero Nikinmaa, Christophe Godin, Anna Lintunen, Pekka Nygren (ed) Proceedings of the 7th international conference on functional-structural plant models (FSPM2013), Saariselkä, Finland, 9–14 June 2013. Vantaa: Finnish Society of Forest Science, pp 279–281

Fournier C, Andrieu B (1998) A 3D architectural and process-based model of maize development. Ann Bot 81(2):233–250

Guo Y, Ma Y-T, Zhan Z-G, Li B-G, Dingkuhn M, Luquet D, De Reffye P (2006) Parameter optimization and field validation of the functional–structural model GreenLab for maize. Ann Bot 97(2):217–230

Hallé F, Oldeman R-A-A, Tomlinson P-B (1978) Tropical trees and forests. Springer Verlag, Berlin, Heidelberg, New-York. 441p

Heuvelink E (1995) Dry matter production in a tomato crop: measurements and simulation. Ann Bot 75(4):369–379

Heuvelink E (1996a) Dry matter partitioning in tomato: validation of a dynamic simulation model. Ann Bot 77(1):71–80

Heuvelink E (1996b) Re-interpretation of an experiment on the role of assimilated transport resistance in partitioning in tomato. Ann Bot 78(4):467–470

Heuvelink E (1999) Evaluation of a dynamic simulation model for tomato crop growth and development. Ann Bot 83(4):413–422

Jourdan C, Rey H (1997) Modelling and simulation of the architecture and development of the oil-palm (*Elaeis guineensis* Jacq.) root system. Plant Soil 190(2):235–246

Kang M, Evers J-B, Vos J, de Reffye P (2008) The derivation of sink functions of wheat organs using the GREENLAB model. Ann Bot 101(8):1099–1108

Lemaire S (2010) Système dynamique de la croissance et du développement de la betterave sucrière (Beta vulgaris L.). AgroParisTech (Ph. D. Thesis)

Lemaire S, Maupas F, Cournède P-H, de Reffye P (2008) A morphogenetic crop model for sugar-beet (beta vulgaris l.). In: International symposium on crop modeling and decision support: ISCMDS 2008, April 19-22, 2008, Nanjing, China, 2008

Ma Y-T, Wen M-P, Guo Y, Li B-G, Cournède P-H, de Reffye P (2008) Parameter optimization and field validation of the functional–structural model GREENLAB for maize at different population densities. Ann Bot 101(8):1185–1194

Mailhol J-C, Revol P, Ruelle P (1996) Pilote: un modèle opérationnel pour déceler l'apparition de stress hydrique. In: ICID 16th international congress on irrigation and drainage: workhop on crop-waterenvironment models, pp 167–182

Marcelis and Gijzen (1998) Evaluation under commercial conditions of a model of prediction of the yield and quality of cucumber fruits. Sci Hortic 76:171–181

Marcelis L-F-M, Heuvelink E, Goudriaanc J (1998) Modelling biomass production and yield of horticultural crops: a review. Sci Hortic 74:83–111

Mathieu A, Cournède P-H, Barthélémy D, de Reffye P (2007) Condition for the generation of rhythms in a discrete dynamic system. Case of a functional structural plant growth model. In: T. Fourcaud and X. P. Zhang. Second international symposium on plant growth modeling, simulation, visualization and applications, PMA06, 13-17 november 2006, Beijing, P.R. China. Los Alamos, IEEE Computer Society, 26–33

Mathieu A, Letort V, Cournède P-H, Zhang B-G, Heuret P, de Reffye P (2012) Oscillations in functional structural plant growth models math. Model Nat Phenom 7(6):47–66

Pagès L, Vercambre G, Drouet J-L, Lecompte F, Collet C, Le Bot J (2004) Root Typ: a generic model to depict and analyse the root system architecture. Plant Soil 258(1):103–119

Rey H (2003) Utilisation de la modélisation 3D pour l'analyse et la simulation du développement et de la croissance végétative d'une plante de tournesol en conditions environnementales fluctuantes (température et rayonnement). Doctoral dissertation, Montpellier, ENSA

Taugourdeau O, Delagrange S, de Reffye P, Messier C (2013) Modelling sugar maple development along its whole ontogeny: modelling hypotheses and calibration methodology. In: Eds. Risto Sievänen, Eero Nikinmaa, Christophe Godin, Anna Lintunen, Pekka Nygren. Proceedings of the 7th international conference on functional-structural plant models (FSPM2013), Saariselkä, Finland, 9–14 June 2013

Urbain A (1920) Influence des matières de réserve de la graine sur le développement des plantes phanérogames. Librairie générale de l'Enseignement, Impr. Nemourienne, 1920

Zhang W, Li B-G (2009) General structural model of crop root system based on the dual-scale automaton. In: Li B.-G., jaeger M. And Guo Y. (Ed) 2010. Proceedings of plant growth modeling, and their applications (PMA09). Beijing, China, November 9–13, IEEE CPS, pp 161–164